

Gauge-Higgs Unification and Radiative Electroweak Symmetry Breaking in Warped Extra Dimensions

Anibal D. Medina ^{a,d}, Nausheen R. Shah ^{b,d}
and Carlos E.M. Wagner ^{b,c,d}

*Department of Astronomy and Astrophysics ^a, Enrico Fermi Institute ^b
and Kavli Institute for Cosmological Physics ^c,*

University of Chicago, 5640 S. Ellis Ave., Chicago, IL 60637, USA

HEP Division, Argonne National Laboratory, 9700 Cass Ave., Argonne, IL 60439, USA ^d

February 8, 2022

Abstract

We compute the Coleman Weinberg effective potential for the Higgs field in RS Gauge-Higgs unification scenarios based on a bulk $SO(5) \times U(1)_X$ gauge symmetry, with gauge and fermion fields propagating in the bulk and a custodial symmetry protecting the generation of large corrections to the T parameter and the coupling of the Z to the bottom quark. We demonstrate that electroweak symmetry breaking may be realized, with proper generation of the top and bottom quark masses for the same region of bulk mass parameters that lead to good agreement with precision electroweak data in the presence of a light Higgs. We compute the Higgs mass and demonstrate that for the range of parameters for which the Higgs boson has Standard Model-like properties, the Higgs mass is naturally in a range that varies between values close to the LEP experimental limit and about 160 GeV. This mass range may be probed at the Tevatron and at the LHC. We analyze the KK spectrum and briefly discuss the phenomenology of the light resonances arising in our model.

1 Introduction

High energy physics experiments in recent years have confirmed the predictions of the Standard Model (SM), a renormalizable, chiral gauge theory based on the group $SU(3)_c \times SU(2)_L \times U(1)_Y$. In particular, the low energy dynamics of fermions and gauge bosons of the theory have been tested with great accuracy. The origin of masses of these fundamental particles, however, remains a mystery. In the SM, masses arise through the vacuum expectation value (vev) of a scalar field doublet, which spontaneously breaks the electroweak (EW) symmetry $SU(2)_L \times U(1)_Y \rightarrow U(1)_{EM}$. A physical, neutral scalar field, the so called Higgs field, appears in the spectrum. Information on the mass of this scalar particle may be obtained through the quantum corrections that it induces to the masses and couplings of the EW gauge bosons. Consistency of the SM predictions with experimental observations is improved for small values of the Higgs mass, m_H , close to the current experimental bound, $m_H \geq 114.4$ GeV [1].

There are several aspects of the mechanism of the origin of mass that demand explanation. On one hand, the scale of the spontaneous symmetry breaking is governed by the size of the scalar mass parameter appearing in the Higgs field effective potential, and is much smaller than the Planck scale, the only known mass scale in nature, besides the dynamical generated QCD scale Λ_{QCD} . Moreover, this scale is associated with a negative value of the squared Higgs mass. There is, however, no dynamical explanation for the origin of the Higgs effective potential, or for the associated breakdown of the EW symmetry. Finally, the hierarchy of the fermion masses of the different generations remains unexplained.

Warped extra dimensions provide a theoretically attractive framework for the solution of the hierarchy problem of the SM. For one extra spatial dimension as in RS1 [2], the curvature k in the extra dimension induces a warp factor on the four dimensional metric, which depends on the position in the extra dimension. The coordinate point, $x_5 = 0$, is associated with a trivial scale factor, leading to natural scales of the order of the Planck scale. The other boundary in the compact dimension, $x_5 = L$, is associated with natural scales that are smaller by an exponential factor $\exp(-kL)$. For natural values of k of the order of the Planck scale and values of $kL \simeq 30$, a Higgs field, located at $x_5 = L$ will naturally acquire a vev of the order of the weak scale. Neither the origin of the breakdown of the EW symmetry, nor the hierarchy of fermion masses, however, are explained by these considerations.

The propagation of fermions and gauge fields in the extra dimension enables a possible explanation for the fermion mass hierarchy. Indeed, chirality of the fermion zero modes is ensured by imposing an orbifold symmetry S_1/Z_2 . Even fields under this orbifold symmetry acquire zero modes whose masses arise from the vev of the Higgs field. For fermion fields, the equations of motion demand that fields of opposite chirality to those having zero modes are odd under the orbifold symmetry and therefore have no zero modes. Finally, localization in the fifth dimension is controlled by a mass parameter c . The variation of c by factors of order one induces exponential variations in the overlap of the fermion wave functions with the Higgs field wave function and therefore on the induced masses for the fermions [3],[4]. Third generation left handed chiral quark fields which couple strongly to the Higgs are associated with a mass parameter $c < 1/2$, and therefore their zero-modes are localized towards the so-called infra-red (IR) brane at $x_5 = L$. On the contrary,

first and second generation left handed chiral fermions have mass parameters $c > 1/2$ and the zero modes are localized towards the so-called ultraviolet (UV) brane at $x_5 = 0$.

Gauge-Higgs unification models [5] provide a solution to the last mysterious aspect of the SM, while leading to a dynamical origin for the Higgs field effective potential. The gauge symmetry of the SM is extended in the bulk and broken at the boundaries. The Higgs is associated with the fifth component of gauge fields in the direction of the broken gauge symmetry. The gauge bosons associated with the broken symmetry are odd under the orbifold symmetry and the fifth component is guaranteed to be even, leading to the presence of massless scalar fields in the theory, with no potential at tree-level. The Coleman-Weinberg Higgs potential is then determined by quantum corrections. For certain values of the fermion mass parameters, this effective potential leads to the Higgs field acquiring a non-zero vev and to the proper generation of gauge boson and fermion masses.

Warped extra dimensions have a rich spectrum of four dimensional Kaluza-Klein (KK) excitations. In particular, after EW symmetry breaking, the KK modes of the weak gauge fields mix with the would-be zero modes, inducing important modifications to the masses and couplings of gauge fields at tree-level. Such large modifications would render the theory inconsistent for values of the gauge field's masses at the reach of the LHC [6]. Recently, it was realized that these large corrections may be prevented by extending the weak gauge symmetry in the bulk of the extra dimension to incorporate the custodial symmetry: $SU(2)_L \times SU(2)_R$ [7]. Moreover, a left-right parity symmetry, P_{LR} is necessary to prevent large corrections to the bottom-quark couplings [8]. A gauge extension of the EW sector of the model to $SO(5) \times U(1)_X$ provides a framework in which gauge-Higgs unification and custodial symmetry are possible. The Higgs potential is fully calculable at one-loop level and a prediction for the Higgs boson mass may be obtained.

Consistency of the theory at the quantum level, however, demands that the possible large corrections to precision electroweak parameters induced by the fermions of the theory be computed. It was recently shown that complete consistency may be obtained for certain values of the mass parameters associated with the fermions of the third generation [9, 10], provided the Higgs remains light, as is expected in Gauge-Higgs unification models.

In this work, we compute the dynamically generated Higgs potential in models similar to the ones previously analyzed in Refs. [9, 10, 11]. The Higgs potential is calculated by means of a generalization of the framework discussed in Ref. [12] and the specifics of our model are complementary to the one discussed in Ref. [11]. We find that a consistent breakdown of the EW symmetry, with a dynamical generation of masses of the gauge bosons and the third generation quarks may only be obtained for certain values of the fermion mass bulk parameters. Interestingly enough, these mass parameters are the same as those demanded by consistency with experimental observations at the quantum level [13]. Moreover, the Higgs boson is predicted to be light, with mass m_H in the range to be probed by the Tevatron and the LHC in the near future.

This article is organized as follows. In section 2 we describe our 5-dimensional (5D) model and derive the gauge boson spectral functions. Furthermore, we analyze the W gauge boson form factor at low energy, defining its coupling to the Higgs field. In section 3 we derive the fermion spectral functions, necessary to compute the loop-induced Higgs effective potential and the fermion mass spectrum. We also compute the top quark form factor at low energy and the associated Yukawa

coupling. Section 4 deals with the explicit computation of the effective potential. In section 5 we present the numerical analysis of the effective potential for the Higgs and the KK spectrum of the theory. We reserve section 6 for our conclusions.

2 5-Dimensional Model and Gauge Fields

We are interested in a 5D gauge theory with gauge group $SO(5) \times U(1)_X$. The geometry of our space-time will be that of RS1 [2], with an orbifolded extra spatial dimension in the interval $x_5 \in [0, L]$. The metric for such a geometry is given by

$$ds^2 = a^2(x_5) \eta_{\mu\nu} dx^\mu dx^\nu - dx_5^2. \quad (1)$$

where $a(x_5) = e^{-kx_5}$. The space spanning the fifth dimension corresponds to a slice of AdS_5 , with branes attached at the two boundary points: $x_5 = 0$ (UV brane) and $x_5 = L$ (IR brane).

We place our gauge fields, $A_M = A_M^\alpha T^\alpha$ and B_M , in the bulk, where T^α are the hermitian generators of the fundamental representation of $SO(5)$ and generically $\text{Tr}[T^\alpha T^\beta] = C(5) \delta^{\alpha,\beta}$. The explicit form of the generators [14] are given in Appendix A.

Our fermions ψ also live in the bulk, and they transform under a representation t^α of $SO(5)$. However, for the moment, we concentrate only on the gauge content of our model. The phenomenologically required fermionic content will be discussed in detail in Section 3.

The 5D action is

$$S_{5D} = \int d^4x \int_0^L dx_5 \sqrt{g} \left(-\frac{1}{4g_5^2} \text{Tr}\{F_{MN} F^{MN}\} - \frac{1}{4g_X^2} G_{MN} G^{MN} + \bar{\psi}(i\Gamma^N D_N - M)\psi \right), \quad (2)$$

where $D_N = \partial_N - iA_N^\alpha t^\alpha - iB_N$ and g_5 and g_X are the 5D dimensionful gauge couplings.

The choice $C(5) = 1$ is a convenient choice, since it allows us to identify the eigenvalues of our generators as the weak isospin, with the four dimensional coupling given by $g^2 = g_5^2/L$. Any other choice for $C(5)$ may be absorbed into a redefinition of the gauge fields or the gauge coupling leaving the physics unchanged.

To construct a realistic 4D low energy theory, we will break the 5D $SO(5) \times U(1)_X$ gauge symmetry down to the subgroup $SO(4) \times U(1)_Y = SU(2)_L \times SU(2)_R \times U(1)_Y$ on the IR brane and to $SU(2)_L \times U(1)_Y$ on the UV brane, where $Y/2 = T^{3R} + Q_X$ is the hypercharge and Q_X is the $U(1)_X$ associated charge which is accommodated to obtain the correct hypercharge. We divide the generators of $SO(5)$ as follows: the generators of $SU(2)_{L,R}$ are denoted by $T^{a_{L,R}}$ and $t^{a_{L,R}}$, while the generators from the coset $SO(5)/SO(4)$ are denoted by $T^{\hat{a}}$ and $t^{\hat{a}}$.

In order to obtain the correct hypercharge and therefore the right Weinberg angle θ_W , we need to rotate the fields $A_M^{3R} \in SU(2)_R$ and $B_M \in U(1)_X$ [15],

$$\begin{pmatrix} A_M^{3R} \\ A_M^Y \end{pmatrix} = \begin{pmatrix} c_\phi & -s_\phi \\ s_\phi & c_\phi \end{pmatrix} \cdot \begin{pmatrix} A_M^{3R} \\ B_M \end{pmatrix} \quad (3)$$

$$c_\phi \equiv \frac{g_5}{\sqrt{g_5^2 + g_X^2}}, \quad s_\phi \equiv \frac{g_X}{\sqrt{g_5^2 + g_X^2}}. \quad (4)$$

where we will enforce A_μ^Y to have even parity, corresponding to the hypercharge gauge boson in the 4D low energy limit. From now on we will drop the prime on A'^{3_R} , and it will be understood that a_R refers to $1_R, 2_R$ and 3_R .

To implement the breaking of $SO(5)$ on the two branes as stated above, we impose the following boundary conditions on the gauge fields:

$$\partial_5 A_\mu^{a_L, Y} = A_\mu^{a_R, \hat{a}} = A_5^{a_L, Y} = 0, \quad x_5 = 0 \quad (5)$$

$$\partial_5 A_\mu^{a_L, a_R, Y} = A_\mu^{\hat{a}} = A_5^{a_L, a_R, Y} = 0, \quad x_5 = L. \quad (6)$$

These boundary conditions lead to 4D scalars $h^{\hat{a}}$ originating from $A_5^{\hat{a}}$. At tree level, the $h^{\hat{a}}$'s have a flat potential and therefore may be thought of as a dual description of Goldstone bosons arising after spontaneous breaking of the global symmetry in 4D. Furthermore, $A_\mu^{a_L}$ and A_μ^Y also have zero modes which will become massive as soon as the $h^{\hat{a}}$'s develop a vev, leading ultimately to electroweak symmetry breaking.

Part of our work consists of obtaining the mass spectrum of the theory in the presence of the vev of $h^{\hat{a}}$. The Higgs forms a bidoublet under $SO(4)$, whose doublet component under $SU(2)_L$ is given by $H \propto (h^{\hat{1}} + ih^{\hat{2}}, h^{\hat{4}} - ih^{\hat{3}})^t$, with charge 0 under the $U(1)_X$. The $SO(4)$ symmetry in principle implies that we can choose any one of the components to be the only non-zero one acquiring a vev. However, we want the scalar Higgs to be a neutral particle, therefore, we choose $\langle h^{\hat{4}} \rangle = h$.

We KK-expand the fields [12],

$$\begin{aligned} A_\mu^a(x, x_5) &= \sum_n f_n^a(x_5, h) A_{\mu, n}(x) & A_5^a(x, x_5) &= \sum_n \frac{\partial_5 f_n^a(x_5, h)}{m_n(h)} h_n(x) \\ A_\mu^{\hat{a}}(x, x_5) &= \sum_n f_n^{\hat{a}}(x_5, h) A_{\mu, n}(x) & A_5^{\hat{a}}(x, x_5) &= \frac{C_h}{a^2(x_5)} h^{\hat{a}}(x) + \sum_n \frac{\partial_5 f_n^{\hat{a}}(x_5, h)}{m_n(h)} h_n(x) \end{aligned} \quad (7)$$

where we have put the explicit dependence on x_5 for the scalars $h^{\hat{a}}(x)$. The normalization constant is chosen so that the scalars are canonically normalized, $C_h = g_5 (\int_0^L a^{-2})^{-1/2}$. We wish to solve for the KK profiles $f_n(x_5, h)$ so that the 5D action may be rewritten in terms of a tower of 4D fields $A_n(x)$ whose kinetic and mass terms, after proper diagonalization, take the form:

$$S_{5D} = \int d^4x \left\{ \frac{1}{2} (\partial_\mu h^{\hat{a}})^2 + \sum_n \left(-\frac{1}{4} [\partial_\mu A_{\nu, n} - \partial_\nu A_{\mu, n}]^2 + \frac{1}{2} m_n^2(h) A_{\mu, n}^2 \right) + \dots \right\} \quad (8)$$

This is done by solving the equations of motion in the presence of the scalar vev, and satisfying the boundary conditions implied by Eqs. (5) and (6).

It turns out that solving the equations of motion in the presence of h is complicated, as these mix the Neumann and Dirichlet modes. However, 5D gauge symmetry relates these solutions to solutions with $h = 0$ [16]. To that end, focusing on the gauge fields, we perform the following gauge transformation on them

$$f^\alpha(x_5, h) T^\alpha = \Omega^{-1}(x_5, h) f^\alpha(x_5, 0) T^\alpha \Omega(x_5, h), \quad (9)$$

where $\Omega(x_5, h)$ is the gauge transformations that removes the vev of h :

$$\Omega(x_5, h) = \exp \left[-i C_h h T^4 \int_0^{x_5} dy a^{-2}(y) \right]. \quad (10)$$

In the $h = 0$ gauge, the gauge KK profiles satisfy the following equation of motion:

$$\left(\partial_5^2 + 2 \frac{a'}{a} \partial_5 + \frac{m_n^2}{a^2} \right) f_n^\alpha(x_5, 0) = 0 \quad (11)$$

which is the same for both Dirichlet and Neumann modes. We call the independent solutions $C(x_5, m_n)$ and $S(x_5, m_n)$, which satisfy the following initial conditions: $C(0, z) = 1$, $C'(0, z) = 0$, $S(0, z) = 0$ and $S'(0, z) = z$. The explicit form of these solutions are given by [17]:

$$C(x_5, z) = \frac{\pi z}{2k} a^{-1}(x_5) \left[Y_0 \left(\frac{z}{k} \right) J_1 \left(\frac{z}{ka(x_5)} \right) - J_0 \left(\frac{z}{k} \right) Y_1 \left(\frac{z}{ka(x_5)} \right) \right] \quad (12)$$

$$S(x_5, z) = \frac{\pi z}{2k} a^{-1}(x_5) \left[J_1 \left(\frac{z}{k} \right) Y_1 \left(\frac{z}{ka(x_5)} \right) - Y_1 \left(\frac{z}{k} \right) J_1 \left(\frac{z}{ka(x_5)} \right) \right] \quad (13)$$

Note from Eq. (10) that for $x_5 = 0$, $f_n^\alpha(x_5, 0) = f_n^\alpha(x_5, h)$. This implies that the gauge KK profiles satisfying the UV boundary conditions given in Eq. (5), can be directly written in terms of the basis functions defined above as

$$\begin{aligned} f_n^{a_L}(x_5, 0) &= C_{n, a_L} C(x_5, m_n), & f_n^{\hat{a}}(x_5, 0) &= C_{n, \hat{a}} S(x_5, m_n) \\ f_n^Y(x_5, 0) &= C_{n, Y} C(x_5, m_n), & f_n^{a_R}(x_5, 0) &= C_{n, a_R} S(x_5, m_n) \end{aligned} \quad (14)$$

where the coefficients $C_{n, \alpha}$ are normalization constants. We can now calculate $f_n^\alpha(x_5, h)$ using Eq. (9). The IR boundary conditions give us a system of algebraic equations for the coefficients $C_{n, \alpha}$. The determinant of this system of equations must vanish to give us a nontrivial solution, and this condition in fact gives us the quantization condition for the masses $m_n(h)$. Using this procedure we find for the gauge bosons:

$$\begin{aligned} &S(L, m_n) S'^3(L, m_n) C'(L, m_n) \times \\ &\left[C'(L, m_n) S(L, m_n) \left(-2 + \sin^2 \left(\frac{\lambda_G h}{f_h} \right) \right) - S'(L, m_n) C(L, m_n) \sin^2 \left(\frac{\lambda_G h}{f_h} \right) \right]^2 \times \\ &\left[C'(L, m_n) S(L, m_n) \left(-2 + (1 + s_\phi^2) \sin^2 \left(\frac{\lambda_G h}{f_h} \right) \right) - S'(L, m_n) C(L, m_n) (1 + s_\phi^2) \sin^2 \left(\frac{\lambda_G h}{f_h} \right) \right] = 0 \end{aligned} \quad (15)$$

where the ‘‘Higgs decay constant’’ is defined as

$$f_h^2 = \frac{1}{g_5^2 \int_0^L dy a^{-2}(y)} \quad (16)$$

and $\lambda_G^2 = 1/2$. Furthermore, using the Wronskian relation

$$S'(x_5, z)C(x_5, z) - C'(x_5, z)S(x_5, z) = z a^{-2}(x_5) \quad (17)$$

we can rewrite the quantization condition in a more convenient form:

$$\begin{aligned} S(L, m_n)S'^3(L, m_n)C'(L, m_n) \left[2a_L^2 C'(L, m_n)S(L, m_n) + m_n \sin^2 \left(\frac{\lambda_G h}{f_h} \right) \right]^2 \times \\ \left[2a_L^2 C'(L, m_n)S(L, m_n) + (1 + s_\phi^2)m_n \sin^2 \left(\frac{\lambda_G h}{f_h} \right) \right] = 0 \end{aligned} \quad (18)$$

Therefore the KK mass spectrum for the W and Z bosons, with the correct Weinberg angle given by $s_\phi^2 \simeq \tan^2 \theta_W \simeq (0.23/0.77) \simeq 0.2987$, is given by the zeroes of the following equations:

$$\begin{aligned} 1 + F_{W,Z}(m_n^2) \sin^2 \left(\frac{\lambda_G h}{f_h} \right) = 0, \quad F_W(z^2) = \frac{z}{2a_L^2 C'(L, z)S(L, z)} \\ F_Z(z^2) = \frac{(1 + s_\phi^2)z}{2a_L^2 C'(L, z)S(L, z)}. \end{aligned} \quad (19)$$

We will identify the first zero of these equations with the masses of W and Z , respectively, and we shall denote the masses of the first excited states as m_{W^1} and m_{Z^1} , associated with the second zeroes of both equations.

We can gain some physical insight if we look at Eq. (18) in the limit $h = 0$. In that case, this equation reduces to,

$$S^4(L, m_n)S'^3(L, m_n)C'^4(L, m_n) = 0 \quad (20)$$

We can identify the zeroes coming from $C'^4(L, m_n) = 0$ with the KK mass spectrum of the 4 gauge bosons belonging to $SU(2)_L \times U(1)_Y$ which are even on both the UV and the IR branes. In the same way, we identify the zeroes of $S'^3(L, m_n) = 0$ with the KK spectrum of the 3 $SU(2)_R$ gauge bosons which are odd on the UV brane and even in the IR brane. $S^4(L, m_n) = 0$ is identified with the KK spectrum of the 4 $SO(5)/SO(4)$ gauge bosons which are odd on both the UV and IR branes. Thus in Eq. (18) we associate the photon KK spectrum with the zeroes of $C'(L, m_n) = 0$.

2.1 Gauge Boson Form Factors at Low Energy

At small momenta, below the scale $\tilde{k} \equiv k \exp(-kL)$, the form factor for the W gauge bosons can be approximated by

$$F_W(-p^2) \approx \frac{g^2 f_h^2}{2p^2}; \quad g = \frac{g_5}{\sqrt{L}}. \quad (21)$$

From the last equation, we can find an analytic expression for the W -mass:

$$m_W^2 \approx \frac{g^2 f_h^2}{2} \sin^2 \left(\frac{\lambda_G h}{f_h} \right) + \mathcal{O}(m_W^4/\tilde{k}^2). \quad (22)$$

From this expression we can calculate the Higgs-W-W coupling, λ_{HWW} , at linear order, by simply taking the derivative of m_W^2 with respect to the vev of h :

$$\lambda_{HWW} = \frac{\partial m_W^2}{\partial h} = g^2 \lambda_G f_h \sin\left(\frac{\lambda_G h}{f_h}\right) \cos\left(\frac{\lambda_G h}{f_h}\right) = g m_w \cos\left(\frac{\lambda_G h}{f_h}\right) \rightarrow g m_w \quad (23)$$

where we used $\lambda_G = 1/\sqrt{2}$ and in the last step note that in the limit $\lambda_G h/f_h \ll 1$ we recover the SM Higgs-W-W coupling. We will discuss the physical implications of the above limiting case in section 5.

3 Fermionic KK profiles

The SM fermions are embedded in full representations of the bulk gauge group. The presence of the $SU(2)_R$ subgroup of the full bulk gauge symmetry ensures the custodial protection of the T parameter [7]. In order to have a custodial protection of the $Zb_L\bar{b}_L$ coupling, the choice $T_R^3(b_L) = T_L^3(b_L)$ has to be enforced [8]. An economical choice is to let the SM $SU(2)_L$ top-bottom doublet arise from a $\mathbf{5}_{2/3}$ of $SO(5) \times U(1)_X$, where the subscript refers to the $U(1)_X$ charge. As discussed in [9], putting the SM $SU(2)_L$ singlet top in the same $SO(5)$ multiplet as the doublet, without further mixing, is disfavored since for the correct value of the top quark mass this leads to a large negative contribution to the T parameter at one loop. Hence we let the right-handed top quark arise from a second $\mathbf{5}_{2/3}$ of $SO(5) \times U(1)_X$. The right handed bottom can come from a $\mathbf{10}_{2/3}$ that allows us to write the bottom Yukawa coupling. For simplicity, and because it allows the generation of the CKM mixing matrix, we make the same choice for the first two quark generations. We therefore introduce in the quark sector three $SO(5)$ multiplets per generation as follows:

$$\begin{aligned} \xi_{1L}^i &\sim Q_{1L}^i = \begin{pmatrix} \chi_{1L}^{u_i}(-, +)_{5/3} & q_L^{u_i}(+, +)_{2/3} \\ \chi_{1L}^{d_i}(-, +)_{2/3} & q_L^{d_i}(+, +)_{-1/3} \end{pmatrix} \oplus u_L^i(-, +)_{2/3}, \\ \xi_{2R}^i &\sim Q_{2R}^i = \begin{pmatrix} \chi_{2R}^{u_i}(-, +)_{5/3} & q_R^{u_i}(-, +)_{2/3} \\ \chi_{2R}^{d_i}(-, +)_{2/3} & q_R^{d_i}(-, +)_{-1/3} \end{pmatrix} \oplus u_R^i(+, +)_{2/3}, \end{aligned} \quad (24)$$

$$\xi_{3R}^i \sim$$

$$T_{1R}^i = \begin{pmatrix} \psi_R^{u_i}(-, +)_{5/3} \\ U_R^{u_i}(-, +)_{2/3} \\ D_R^{u_i}(-, +)_{-1/3} \end{pmatrix} \oplus T_{2R}^i = \begin{pmatrix} \psi_R^{u_i}(-, +)_{5/3} \\ U_R^{u_i}(-, +)_{2/3} \\ D_R^{u_i}(+, +)_{-1/3} \end{pmatrix} \oplus Q_{3R}^i = \begin{pmatrix} \chi_{3R}^{u_i}(-, +)_{5/3} & q_R^{u_i}(-, +)_{2/3} \\ \chi_{3R}^{d_i}(-, +)_{2/3} & q_R^{d_i}(-, +)_{-1/3} \end{pmatrix},$$

where we show the decomposition under $SU(2)_L \times SU(2)_R$, and explicitly write the $U(1)_{EM}$ charges. The Q^i 's are bidoublets of $SU(2)_L \times SU(2)_R$, with $SU(2)_L$ acting vertically and $SU(2)_R$ acting horizontally. The T_1^i 's and T_2^i 's transform as $(\mathbf{3}, \mathbf{1})$ and $(\mathbf{1}, \mathbf{3})$ under $SU(2)_L \times SU(2)_R$, respectively, while u^i and u^i are $SU(2)_L \times SU(2)_R$ singlets. The superscripts, $i = 1, 2, 3$, label the three generations.

We also show the parities on the indicated 4D chirality, where $-$ and $+$ stands for odd and even parity conditions and the first and second entries in the bracket correspond to the parities in the UV and IR branes respectively. Let us stress that while odd parity is equivalent to a Dirichlet boundary condition, the even parity is a linear combination of Neumann and Dirichlet boundary conditions, that is determined via the fermion bulk equations of motion as discussed below.

The boundary conditions for the opposite chirality fermion multiplet can be read off the ones above by a flip in both chirality and boundary condition, $(-, +)_L \rightarrow (+, -)_R$ for example. In the absence of mixing among multiplets satisfying different boundary conditions, the SM fermions arise as the zero-modes of the fields obeying $(+, +)$ boundary conditions. The remaining boundary conditions are chosen so that $SU(2)_L \times SU(2)_R$ is preserved on the IR brane and so that mass mixing terms, necessary to obtain the SM fermion masses after EW symmetry breaking, can be written on the IR brane. Consistency of the above parity assignments with the original orbifold Z_2 symmetry at the IR brane will be discussed in Appendix B.

As remarked above, the zero-mode fermions can acquire EW symmetry breaking masses through mixing effects. The most general $SU(2)_L \times SU(2)_R \times U(1)_X$ invariant mass Lagrangian at the IR brane – compatible with the boundary conditions – is, in the quark sector,

$$\mathcal{L}_m = 2\delta(x_5 - L) \left[\bar{u}'_L M_{B_1} u_R + \bar{Q}_{1L} M_{B_2} Q_{3R} + \bar{Q}_{1L} M_{B_3} Q_{2R} + \text{h.c.} \right], \quad (25)$$

where M_{B_1} , M_{B_2} and M_{B_3} are dimensionless 3×3 matrices, and matrix notation is employed. In Appendix B we will show how these mass terms may be generated from an $SO(5)$ invariant Lagrangian using the spurion formalism. To prevent negative corrections to the T parameter [18], [9, 10], we will take M_{B_3} to be the null matrix. In Appendix C however we briefly discuss the modifications of the effective Higgs potential induced by a non-zero value of M_{B_3} . Moreover since the Higgs effective potential is most sensitive to the third generation, we will concentrate on this one, discarding family indices.

With the introduction of these brane mixing terms, the different multiplets are now related via the equations of motion. In the case of a mass term involving $\bar{\Psi}_L^1 \Psi_R^2$, with the fields having profile functions g_L and h_R , the odd parity profile g_R on the IR brane is related to h_R :

$$\int_{L-\epsilon}^{L+\epsilon} (\partial_5 g_R) dx_5 = \int_{L-\epsilon}^{L+\epsilon} (2M h_R - g_R) \delta(x_5 - L) dx_5. \quad (26)$$

The odd parity we demand at the IR brane implies a Dirichlet boundary condition for the function g_R . Therefore, we can rewrite:

$$\lim_{\epsilon \rightarrow 0} g_R(L - \epsilon) = -M h_R(L), \quad (27)$$

and, similarly:

$$\lim_{\epsilon \rightarrow 0} h_L(L - \epsilon) = M g_L(L). \quad (28)$$

Eq. (27) and (28) can now be reinterpreted as the new boundary conditions for the profiles at the IR brane.

The fermions, like the gauge bosons, can be expanded in their KK basis:

$$\psi_L(x, x_5) = \sum_n f_{L,n}(x_5, h) \psi_{L,n}(x), \quad \psi_R(x, x_5) = \sum_n f_{R,n}(x_5, h) \psi_{R,n}(x). \quad (29)$$

In the $h = 0$ gauge, we redefine $\hat{\psi} = a^2(x_5)\psi$ and we write our vector-fermionic fields in terms of chiral fields. We can KK decompose the fermionic chiral components as,

$$\hat{\psi}_{L,R} = \sum_{n=0}^{\infty} \psi_{L,R}^n(x^\mu) \hat{f}_{L,R,n}(x_5) \quad (30)$$

where \hat{f} is normalized by:

$$\int_0^L dx_5 a^{-1}(x_5) \hat{f}_n \hat{f}_m = \delta_{m,n}. \quad (31)$$

Therefore the profile function for the zero mode fermion corresponds to $a^{-1/2}(x_5)\hat{f}_0$.

From the 5D action, Eq. (2), concentrating on the free fermionic fields, we can derive the following first order coupled equations of motion for $\hat{f}_{L,R,n}$,

$$(\partial_5 + M)\hat{f}_{R,n} = (z/a(x_5))\hat{f}_{L,n}; \quad (\partial_5 - M)\hat{f}_{L,n} = -(z/a(x_5))\hat{f}_{R,n} \quad (32)$$

We see from Eq. (32) that we can redefine $\tilde{f}_{R,L,n} = e^{-Mx_5}\hat{f}_{R,L,n}$ and relate the opposite chiral component of the same vector-like field by $\tilde{f}_{R,n} = (-a(x_5)/z)\partial_5\tilde{f}_{L,n}$. For the left handed field having Dirichlet boundary conditions on the UV brane, we can derive a second order equation for the chiral component $\tilde{f}_{L,n}$:

$$\left[\partial_5^2 + \left(\frac{a'}{a} + 2M \right) \partial_5 + \frac{z^2}{a^2} \right] \tilde{f}_{L,n} = 0 \quad (33)$$

the solution of which we shall call $\tilde{S}_M(x_5, z)$, with boundary conditions $\tilde{S}_M(0, z) = 0$, $\tilde{S}'_{\pm M}(0, z) = z$.

Similarly, we can redefine $\tilde{f}_{R,L,n} = e^{Mx_5}\hat{f}_{R,L,n}$ and then relate the opposite chirality via $\tilde{f}_{L,n} = (a(x_5)/z)\partial_5\tilde{f}_{R,n}$. If the right-handed field fulfills Dirichlet boundary conditions on the UV-brane, we can write the equation of motion for $\tilde{f}_{R,n}$:

$$\left[\partial_5^2 + \left(\frac{a'}{a} - 2M \right) \partial_5 + \frac{z^2}{a^2} \right] \tilde{f}_{R,n} = 0. \quad (34)$$

We shall correspondingly denote the solution to this equation with $\tilde{S}_{-M}(x_5, z)$, fulfilling the boundary conditions $\tilde{S}_{-M}(0, z) = 0$, $\tilde{S}'_{-M}(0, z) = z$.

As emphasized before, the solutions of the opposite chirality, are related to these solutions via the the first order equations of motion, Eqs. (32), which we rewrite as $\dot{\tilde{S}}_{\pm M}(x_5, z) = \mp(a(x_5)/z)\partial_5\tilde{S}_{\pm M}(x_5, z)$. Here $M = -ck$, and the \pm is chosen depending on whether we want an odd (-) boundary condition on the UV brane for the left-handed or right-handed fermionic field. The solution to Eq. (33) is given by [17]:

$$\tilde{S}_M(x_5, z) = \frac{\pi z}{2k} a^{-c-\frac{1}{2}}(x_5) \left[J_{\frac{1}{2}+c} \left(\frac{z}{k} \right) Y_{\frac{1}{2}+c} \left(\frac{z}{ka(x_5)} \right) - Y_{\frac{1}{2}+c} \left(\frac{z}{k} \right) J_{\frac{1}{2}+c} \left(\frac{z}{ka(x_5)} \right) \right]. \quad (35)$$

The solution for Eq. (34) is given by Eq. (35), with the replacement $c \rightarrow -c$.

Before proceeding with the gauge transformations as was done with the gauge fields, we would like to discuss what is required of the gauge transformation for the fermions. The boundary conditions are explicitly given on the physical fermion which is an isospin eigenvector. Hence, the first step is to identify the different components of the vector ψ with the doublets, triplets and singlets as required from Eq. (24). Second, we need to assign functions to the different components of the multiplets consistent with the boundary conditions for the fermions given in Eq. (24). The basis $f_{L,R,n}$ and $\tilde{f}_{L,R,n}$ are simply related by exponentials, therefore, the functions $f_{L,R,n}$, given by $S_{\pm M}$ and $\dot{S}_{\pm M}$, are related to $\tilde{f}_{L,R,n}$ via $S_{\pm M}(\dot{S}_{\pm M}) = a^{-2}(x_5) \exp[\pm Mx_5] \tilde{S}_{\pm M}(\dot{\tilde{S}}_{\pm M})$. Odd and even solutions (S or \dot{S}) can then be assigned to the component functions of the multiplets ξ_{1L} , ξ_{2R} and ξ_{3R} , depending on the boundary parities. For example, for a left handed component having boundary conditions $(-, +)_L$ or $(-, -)_L$, since the function is odd at the UV brane, we assign a solution \dot{S}_M to that component of the left-handed multiplet. If the boundary condition is $(+, +)_L$, or $(+, -)_L$ we need to look at the chiral companion $(-, -)_R$ or $(-, +)_R$. In this case, our right handed fermion is odd on the UV brane. The relationship between the left and the right handed components are as defined above via derivatives. Therefore, we assign \dot{S}_{-M} to the left-handed fermion. Following this procedure, we can assign either $S_{\pm M}$ or $\dot{S}_{\pm M}$ to each component of the multiplets. This procedure defines our three fermion multiplets in the $h = 0$ gauge as the vector functions:

$$\begin{aligned}
f_{1,L}(x_5, 0) &= \begin{bmatrix} C_1 S_{M_1} \\ C_2 S_{M_1} \\ C_3 \dot{S}_{-M_1} \\ C_4 \dot{S}_{-M_1} \\ C_5 S_{M_1} \end{bmatrix} & f_{3,R}(x_5, 0) &= \begin{bmatrix} C_{11} S_{-M_3} \\ C_{12} S_{-M_3} \\ C_{13} S_{-M_3} \\ C_{14} S_{-M_3} \\ C_{15} S_{-M_3} \\ C_{16} S_{-M_3} \\ C_{17} S_{-M_3} \\ C_{18} S_{-M_3} \\ C_{19} S_{-M_3} \\ C_{20} \dot{S}_{M_3} \end{bmatrix} \\
f_{2,R}(x_5, 0) &= \begin{bmatrix} C_6 S_{-M_2} \\ C_7 S_{-M_2} \\ C_8 S_{-M_2} \\ C_9 S_{-M_2} \\ C_{10} \dot{S}_{M_2} \end{bmatrix} & &
\end{aligned} \tag{36}$$

where, as for the gauge bosons, the C_i are normalization constants. The opposite chiralities have opposite boundary conditions and can be read from these ones.

The boundary conditions as written above, for example, for the vector components of $f_{1,L}(x_5, 0)$ are the boundary conditions on the isospin eigenvector with charges $(+1/2, +1/2)$, $(-1/2, +1/2)$, $(+1/2, -1/2)$, $(-1/2, -1/2)$, $(0, 0)$ under $SU(2)_L \times SU(2)_R$, respectively. However, in the basis of our generators, the eigenvector with spin $+1/2$ under $SU(2)_L$, for example, is given by:

$$\hat{e} = \frac{1}{\sqrt{2}} \begin{bmatrix} i \\ -1 \\ 0 \\ 0 \\ 0 \end{bmatrix}. \tag{37}$$

To simplify matters, so that the boundary conditions can be taken to be on the eigenvector:

$$\hat{e} = \begin{bmatrix} 1 \\ 0 \\ 0 \\ 0 \\ 0 \end{bmatrix} \quad (38)$$

the transformation Ω needs to be in the basis consistent with Eq. (38), or we can also think about this as changing the fermion vector functions given in Eq. (36) to the basis of our generators. This means that we have to first understand how the eigenvectors of $T^{3R,L}$ decompose in the canonical basis for both the $\mathbf{5}_{2/3}$ and the $\mathbf{10}_{2/3}$.

For the $\mathbf{5}_{2/3}$ fermions, the basis transformation for ξ_{1L} , ξ_{2R} is given by

$$A = \frac{1}{\sqrt{2}} \begin{pmatrix} -i & -1 & 0 & 0 & 0 \\ 0 & 0 & -i & 1 & 0 \\ 0 & 0 & i & 1 & 0 \\ -i & 1 & 0 & 0 & 0 \\ 0 & 0 & 0 & 0 & \sqrt{2} \end{pmatrix} \quad (39)$$

For $\mathbf{10}_{2/3}$, the transformation matrix for ξ_{3R} is given by

$$B = \frac{1}{\sqrt{2}} \begin{pmatrix} i & 1 & 0 & 0 & 0 & 0 & 0 & 0 & 0 & 0 \\ 0 & 0 & -i & 1 & 0 & 0 & 0 & 0 & 0 & 0 \\ 0 & 0 & -i & -1 & 0 & 0 & 0 & 0 & 0 & 0 \\ -i & 1 & 0 & 0 & 0 & 0 & 0 & 0 & 0 & 0 \\ 0 & 0 & 0 & 0 & -1 & i & 0 & 0 & 0 & 0 \\ 0 & 0 & 0 & 0 & 0 & 0 & \sqrt{2} & 0 & 0 & 0 \\ 0 & 0 & 0 & 0 & 1 & i & 0 & 0 & 0 & 0 \\ 0 & 0 & 0 & 0 & 0 & 0 & 0 & -1 & i & 0 \\ 0 & 0 & 0 & 0 & 0 & 0 & 0 & 0 & 0 & \sqrt{2} \\ 0 & 0 & 0 & 0 & 0 & 0 & 0 & 1 & i & 0 \end{pmatrix} \quad (40)$$

Therefore, once the UV boundary conditions define the vectors as in Eq. (36), we change bases to be able to implement the gauge transformation and then transform back so that the IR boundary conditions can be imposed. Using the transformations defined in Eq. (39) and (40), we can write the final fermion vector functions in the presence of the vev of h as:

$$f_{1,L}(x_5, h) = A\Omega A^{-1}f_{1,L}(x_5, 0) \quad (41)$$

$$f_{2,R}(x_5, h) = A\Omega A^{-1}f_{2,R}(x_5, 0) \quad (42)$$

$$f_{3,R}(x_5, h) = B\Omega B^{-1}f_{3,R}(x_5, 0) \quad (43)$$

Applying the boundary conditions at $x_5 = L$, taking into account the mass mixing terms from

Eq. (25) and using the procedure defined in Eqs. (27) and (28), we derive the conditions on $f(L, h)$:

$$\begin{aligned} f_{1,R}^{1,\dots,4} + M_{B_2} f_{3,R}^{1,\dots,4} &= 0 & f_{1,R}^5 + M_{B_1} f_{2,R}^5 &= 0 & f_{2,L}^{1,\dots,4} &= 0 \\ f_{3,L}^{1,\dots,4} - M_{B_2} f_{1,L}^{1,\dots,4} &= 0 & f_{2,L}^5 - M_{B_1} f_{1,L}^5 &= 0 & f_{3,L}^{5,\dots,10} &= 0 \end{aligned} \quad (44)$$

where the superscripts denote the vector components.

Asking that the determinant of this system of equations vanishes so that we get a non-trivial solution, we notice that all dependence on the prefactors $a^{-3/2}(x_5) \exp[\pm M x_5]$ relating $S_{\pm M}, \dot{S}_{\pm M}$ and $\tilde{S}_{\pm M}, \dot{\tilde{S}}_{\pm M}$ drops out, and thus we conclude that one of the following equations should vanish:

$$\tilde{S}'^3_{-M_2} = 0 \quad (45)$$

$$\tilde{S}'^5_{-M_3} = 0 \quad (46)$$

$$\left[M_{B_2}^2 \tilde{S}_{M_1} \tilde{S}_{-M_3} - \frac{a_L^2}{z^2} \tilde{S}'_{M_1} \tilde{S}'_{-M_3} \right]^2 = 0 \quad (47)$$

$$2\tilde{S}_{M_3} \left[M_{B_2}^2 \tilde{S}_{-M_3} \tilde{S}'_{-M_1} + \tilde{S}_{-M_1} \tilde{S}'_{-M_3} \right] - M_{B_2}^2 \tilde{S}'_{-M_1} \sin^2 \left(\frac{\lambda_F h}{f_h} \right) = 0 \quad (48)$$

$$\begin{aligned} & 2 \left[M_{B_1}^2 \tilde{S}_{M_1} \left(-1 + \tilde{S}_{M_2} \tilde{S}_{-M_2} \right) \left(M_{B_2}^2 \tilde{S}_{-M_3} \tilde{S}'_{-M_1} + \tilde{S}_{-M_1} \tilde{S}'_{-M_3} \right) + \right. \\ & \left. \tilde{S}_{M_2} \tilde{S}'_{-M_2} \left(M_{B_2}^2 \left(-1 + \tilde{S}_{M_1} \tilde{S}_{-M_1} \right) \tilde{S}_{-M_3} - \frac{a_L^2}{z^2} \tilde{S}_{-M_1} \tilde{S}'_{M_1} \tilde{S}'_{-M_3} \right) \right] + \\ & \left[M_{B_2}^2 \tilde{S}_{M_2} \tilde{S}_{-M_3} \tilde{S}'_{-M_2} + M_{B_1}^2 \left(2M_{B_2}^2 \tilde{S}_{M_1} \tilde{S}_{-M_3} \tilde{S}'_{-M_1} + \tilde{S}'_{-M_3} + 2\tilde{S}_{M_1} \tilde{S}_{-M_1} \tilde{S}'_{-M_3} - \right. \right. \\ & \left. \left. \tilde{S}_{M_2} \tilde{S}_{-M_2} \tilde{S}'_{-M_3} \right) \right] \sin^2 \left(\frac{\lambda_F h}{f_h} \right) - M_{B_1}^2 \tilde{S}'_{-M_3} \sin^4 \left(\frac{\lambda_F h}{f_h} \right) = 0 \end{aligned} \quad (49)$$

where for simplicity we did not write the dependence on L and z and furthermore, we have used the Crowian:

$$- \dot{\tilde{S}}_M(x_5, z) \dot{\tilde{S}}_{-M}(x_5, z) + \tilde{S}_M(x_5, z) \tilde{S}_{-M}(x_5, z) = 1. \quad (50)$$

In the following, and for simplicity, we shall omit the tildes and refer to the solutions $\tilde{S}_{\pm M}$ by $S_{\pm M}$.

The same value $\lambda_F = 1/\sqrt{2}$ is found in the fermionic case, so from now on $\lambda = \lambda_G = \lambda_F$. The solutions to Eqs. (45), (46) and (47) can be interpreted as the KK spectrum of exotic fermions. We shall name these states E_3 , E_2 and E_1 , respectively. Eq. (48) is the KK mass spectrum for the bottom quark and Eq. (49) gives the KK spectrum for the top quark.

We can rewrite Eqs. (48) and (49) in the same form as the gauge bosons:

$$1 + F_b(m_n^2) \sin^2 \left(\frac{\lambda h}{f_h} \right) = 0, \quad (51)$$

$$1 + F_{t_1}(m_n^2) \sin^2 \left(\frac{\lambda h}{f_h} \right) + F_{t_2}(m_n^2) \sin^4 \left(\frac{\lambda h}{f_h} \right) = 0 \quad (52)$$

where

$$F_b(z^2) = -\frac{M_{B_2}^2 S'_{-M_1}}{2S_{M_3}(M_{B_2}^2 S_{-M_3} S'_{-M_1} + S_{-M_1} S'_{-M_3})} \quad (53)$$

$$F_{t_1}(z^2) = \frac{F_1(z^2)}{F_d(z^2)} \quad (54)$$

$$F_{t_2}(z^2) = \frac{F_2(z^2)}{F_d(z^2)}, \quad (55)$$

$$F_1(z^2) = M_{B_2}^2 S_{M_2} S_{-M_3} S'_{-M_2} + M_{B_1}^2 [2M_{B_2}^2 S_{M_1} S_{-M_3} S'_{-M_1} + S'_{-M_3} + 2S_{M_1} S_{-M_1} S'_{-M_3} - S_{M_2} S_{-M_2} S'_{-M_3}] \quad (56)$$

$$F_2(z^2) = -M_{B_1}^2 S'_{-M_3} \quad (57)$$

$$F_d(z^2) = 2 [M_{B_1}^2 S_{M_1} (-1 + S_{M_2} S_{-M_2}) (M_{B_2}^2 S_{-M_3} S'_{-M_1} + S_{-M_1} S'_{-M_3}) + S_{M_2} S'_{-M_2} \left(M_{B_2}^2 (-1 + S_{M_1} S_{-M_1}) S_{-M_3} - \frac{a_L^2}{z^2} S_{-M_1} S'_{M_1} S'_{-M_3} \right)] \quad (58)$$

Equations (19), (51) and (52) are the starting point for computing the one-loop effective potential for the scalars $h^{\hat{a}}$.

It is physically very illuminating to interpret the origin of the fermionic resonances if we contemplate the fermionic determinant in the case $h = 0$:

$$\begin{aligned} S_{M_3} &= 0 & S_{M_2} S'_{M_1} + M_{B_1}^2 S_{M_1} S'_{M_2} &= 0 \\ S_{-M_3}^5 &= 0 & (M_{B_2}^2 S_{-M_3} S'_{-M_1} + S_{-M_1} S'_{-M_3})^2 &= 0 \\ S_{-M_2}^4 &= 0 & (M_{B_2}^2 S_{M_1} S_{-M_3} - \frac{a_L^2}{z^2} S'_{M_1} S'_{-M_3})^2 &= 0 \end{aligned} \quad (59)$$

We recall that the way we defined the initial fermionic functions ($S_{\pm M}$) was via the boundary condition on the UV brane and the chirality. However, since we are in the $h = 0$ gauge, we can use the boundary conditions on the IR brane to further give us the final equations the functions have to satisfy:

$$\begin{aligned} (-, -)_L &\Rightarrow S_M(L) = 0, & (-, -)_R &\Rightarrow S_{-M}(L) = 0 \\ (-, +)_L &\rightarrow S_M \rightarrow (+, -)_R \Rightarrow S'_M(L) = 0, & (-, +)_R &\rightarrow S_{-M} \rightarrow (+, -)_L \Rightarrow S'_{-M}(L) = 0 \end{aligned} \quad (60)$$

We can now interpret Eq. (59) in a simple way: the first equation in the first line provides the mass spectrum for the singlet right handed bottom. This with the first equation in the second line provide the mass spectrum of the triplet components T_{1R} , T_{2R} of ξ_{3R} . The second equation in the first line may be identified with the mass spectrum of the singlet t_R and its modification from the mixing mass term with u'_L . It can be shown from this equation that the light top resonances will be mostly the KK modes of the right handed top. From the first equation in the third line we

get the mass spectrum for Q_{2R} . Additionally we can also see here the mixing of the bidoublets Q_1 and Q_3 . The second equation in the second line is related to the mass spectrum for the $(t_L, b_L)^t$ doublet and its mixing with $(q_{3L}^u, q_{3L}^d)^t$. The second equation in the third line may be identified as the spectrum of a new fermionic state coming from the doublet-doublet mixing between $(\chi_{1L}^u, \chi_{1L}^d)^t$ and $(\chi_{2L}^u, \chi_{2L}^d)^t$.

3.1 Top Mass and Yukawa Coupling at Low Energy

At small momenta, the solution to Eq. (35) takes the form:

$$\tilde{S}_M \approx z \int_0^{x_5} a^{-1}(x_5) e^{-2My} dy + \mathcal{O}(z^3). \quad (61)$$

Replacing this in Eq. (49), keeping only quadratic terms in z and for simplicity neglecting the small M_{B2} effects, we find that the top quark spectral equation reduces to:

$$A \left(\frac{z}{\tilde{k}} \right)^2 + M_{B1}^2 \left[1 + B \left(\frac{z}{\tilde{k}} \right)^2 \right] \sin^2 \left(\frac{\lambda h}{f_h} \right) - M_{B1}^2 \sin^4 \left(\frac{\lambda h}{f_h} \right) = 0, \quad (62)$$

where A and B are coefficients given by:

$$A = -\frac{(\frac{1}{2} + c_1) + M_{B1}^2(\frac{1}{2} + c_2)}{2(\frac{1}{4} - c_1^2)(\frac{1}{2} + c_2)} \quad ; \quad B = \frac{(\frac{1}{4} - c_2^2) - \frac{1}{2}(\frac{1}{4} - c_1^2)}{2(\frac{1}{4} - c_1^2)(\frac{1}{4} - c_2^2)}. \quad (63)$$

Solving Eq. (62) for z^2 , we find that the top mass takes the form

$$\left(\frac{m_t}{\tilde{k}} \right)^2 \approx -\frac{M_{B1}^2 \sin^2 \left(\frac{\lambda h}{f_h} \right) \cos^2 \left(\frac{\lambda h}{f_h} \right)}{A + M_{B1}^2 B \sin^2 \left(\frac{\lambda h}{f_h} \right)} + \mathcal{O}(m_t^3/\tilde{k}^3), \quad (64)$$

which can also be written as

$$\left(\frac{m_t}{\tilde{k}} \right)^2 \approx \frac{2M_{B1}^2 \sin^2 \left(\frac{\lambda h}{f_h} \right) \cos^2 \left(\frac{\lambda h}{f_h} \right) (\frac{1}{4} - c_1^2)(\frac{1}{4} - c_2^2)}{(\frac{1}{2} - c_2)(\frac{1}{2} + c_1) + M_{B1}^2 \left[(\frac{1}{4} - c_2^2) \cos^2 \left(\frac{\lambda h}{f_h} \right) + \frac{1}{2}(\frac{1}{4} - c_1^2) \sin^2 \left(\frac{\lambda h}{f_h} \right) \right]}. \quad (65)$$

This expression is similar to the one obtained in a related model in Ref. [11]. From this expression we can calculate the Yukawa coupling of the top, Y_t , at linear order, by simply taking the derivative of m_t with respect to h :

$$Y_t = \sqrt{2} \frac{\partial m_t}{\partial h} \simeq \frac{m_t g}{m_W \sqrt{2}} \frac{\cos \left(\frac{2\lambda h}{f_h} \right)}{\cos \left(\frac{\lambda h}{f_h} \right)}, \quad (66)$$

where we note that in the limit $\lambda h/f_h \ll 1$, we recover the SM top Yukawa coupling.

4 Coleman–Weinberg potential for $h^{\hat{a}}$ in 5D

The Coleman–Weinberg potential in 5D KK theories (see for instance [12]) takes the form:

$$V(h) = \sum_r \pm \frac{N_r}{(4\pi)^2} \int_0^\infty dp p^3 \log[\rho(-p^2)]. \quad (67)$$

Here N is the number of degrees of freedom of a given particle, \pm depends on whether we are considering bosons or fermions and $\rho(z^2)$ is the spectral function encoding the spectrum in the presence of h . We showed in the previous section that in the 5D framework the spectral functions encoding the KK spectrum in the presence of the Higgs vev are given by:

$$\begin{aligned} \rho_W(z^2) &= 1 + F_W(z^2) \sin^2\left(\frac{\lambda h}{f_h}\right) & \rho_Z(z^2) &= 1 + F_Z(z^2) \sin^2\left(\frac{\lambda h}{f_h}\right), \\ \rho_b(z^2) &= 1 + F_b(z^2) \sin^2\left(\frac{\lambda h}{f_h}\right) & \rho_t(z^2) &= 1 + F_{t_1}(z^2) \sin^2\left(\frac{\lambda h}{f_h}\right) + F_{t_2}(z^2) \sin^4\left(\frac{\lambda h}{f_h}\right) \end{aligned} \quad (68)$$

Thus, the scalar potential for the pseudo-Goldstone can be written as:

$$\begin{aligned} V(h) &= \int_0^\infty dp p^3 \left(-\frac{12}{(4\pi)^2} \left\{ \log \left[1 + F_{t_1}(-p^2) \sin^2\left(\frac{\lambda h}{f_h}\right) + F_{t_2}(-p^2) \sin^4\left(\frac{\lambda h}{f_h}\right) \right] + \right. \right. \\ &\quad \left. \left. \log \left[1 + F_b(-p^2) \sin^2\left(\frac{\lambda h}{f_h}\right) \right] \right\} + \frac{6}{(4\pi)^2} \log \left[1 + F_W(-p^2) \sin^2\left(\frac{\lambda h}{f_h}\right) \right] + \right. \\ &\quad \left. \frac{3}{(4\pi)^2} \log \left[1 + F_Z(-p^2) \sin^2\left(\frac{\lambda h}{f_h}\right) \right] \right) \end{aligned} \quad (69)$$

The form factors F_W and F_Z for the gauge bosons are given by Eq. (19), and F_b , F_{t_1} and F_{t_2} for the fermions are given by Eq. (51) and (52). We note here that the main contribution to the potential from the fermionic sector is due to the top quark. Therefore, the first two fermion multiplets, ξ_1 and ξ_2 are the most important for fixing the Higgs potential.

5 Numerical Results

Our goal is to find a non-trivial minimum of the Higgs effective potential that will break $SU(2)_L \times U(1)_Y$ down to $U(1)_{EM}$. The relevant parameters which control the model are M_{B_1} , M_{B_2} , c_1 , c_2 , c_3 and kL , where $M_1 = -c_1 k$, $M_2 = -c_2 k$, $M_3 = -c_3 k$ and L is the length of the extra dimension. Looking at the potential we immediately see that $\sin(\lambda h/f_h) = 1$ is a non-trivial extremum. When $(\lambda h/f_h) = 0$ corresponds to a maximum, this extremum can be a minimum. However this would lead to a non-standard effective low-energy theory, since as seen from the form factors, and from Eq. (23), the Higgs coupling to the gauge bosons vanishes at linear order¹. Therefore, we shall concentrate

¹Couplings of higher order in Higgs field do not vanish, but the interpretation of such a theory goes beyond the scope of this work

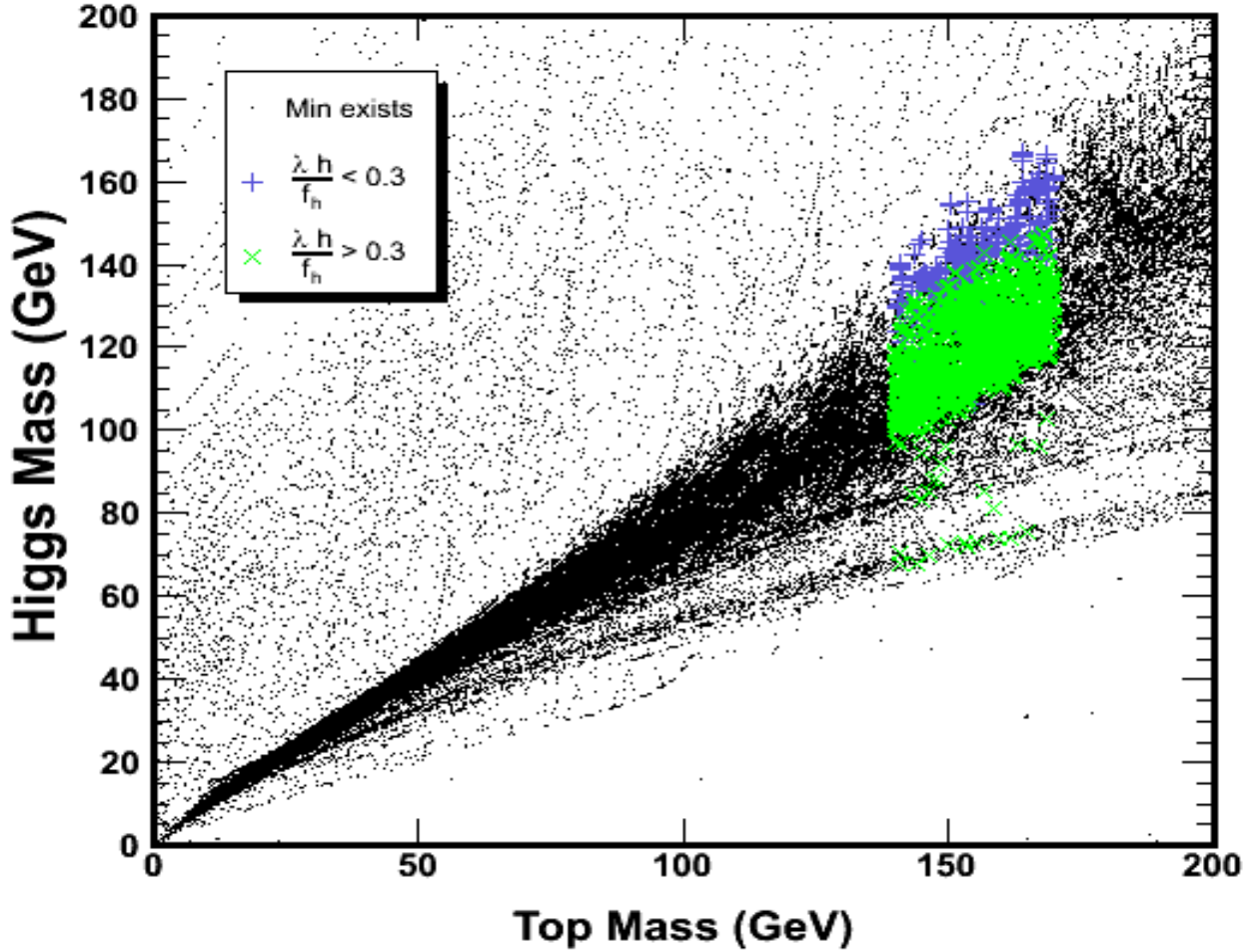


Figure 1: Higgs Mass vs top mass in GeV. Blue (dark gray) crosses represent the linear regime, green (light gray) x's the non-linear regime and black dots where a minimum for the effective potential exists.

only in the regions of parameter space such that $0 < \sin(\lambda h/f_h) < 1$ with $0 < \lambda h/f_h < \pi/2$. After obtaining a non-trivial minimum, we calculate k by finding the first zero of Eq. (19) and setting this mass equal to the W mass [19]. This is the mass that the W zero-mode gets from interacting with the Higgs vev. Since the relationship between the Z and the W form factors remains the same as in the SM, we also recover a consistent mass for the Z boson.

Having obtained k , we calculate the top-quark mass, given by the first zero of Eq. (52), and demand that its value is in the phenomenological range $m_{top} \in [140, 170]$ GeV. We take such a wide range since we consider the result of our calculation to be associated with the running top-quark mass evaluated at a scale of the order of the weak scale. Due to the strong gauge coupling, the running top-quark mass varies rapidly between values of $m_{top} \sim 140$ GeV, for a scale of the order of a few TeV, to values of $m_{top} \sim 165$ GeV, for a scale of order of the top quark pole mass M_t . Furthermore, we also calculate the bottom quark mass, given by the first zero of Eq. (51), and demand it to be in the phenomenological range $m_{bottom} \in [2, 4]$ GeV. The Higgs mass is given by

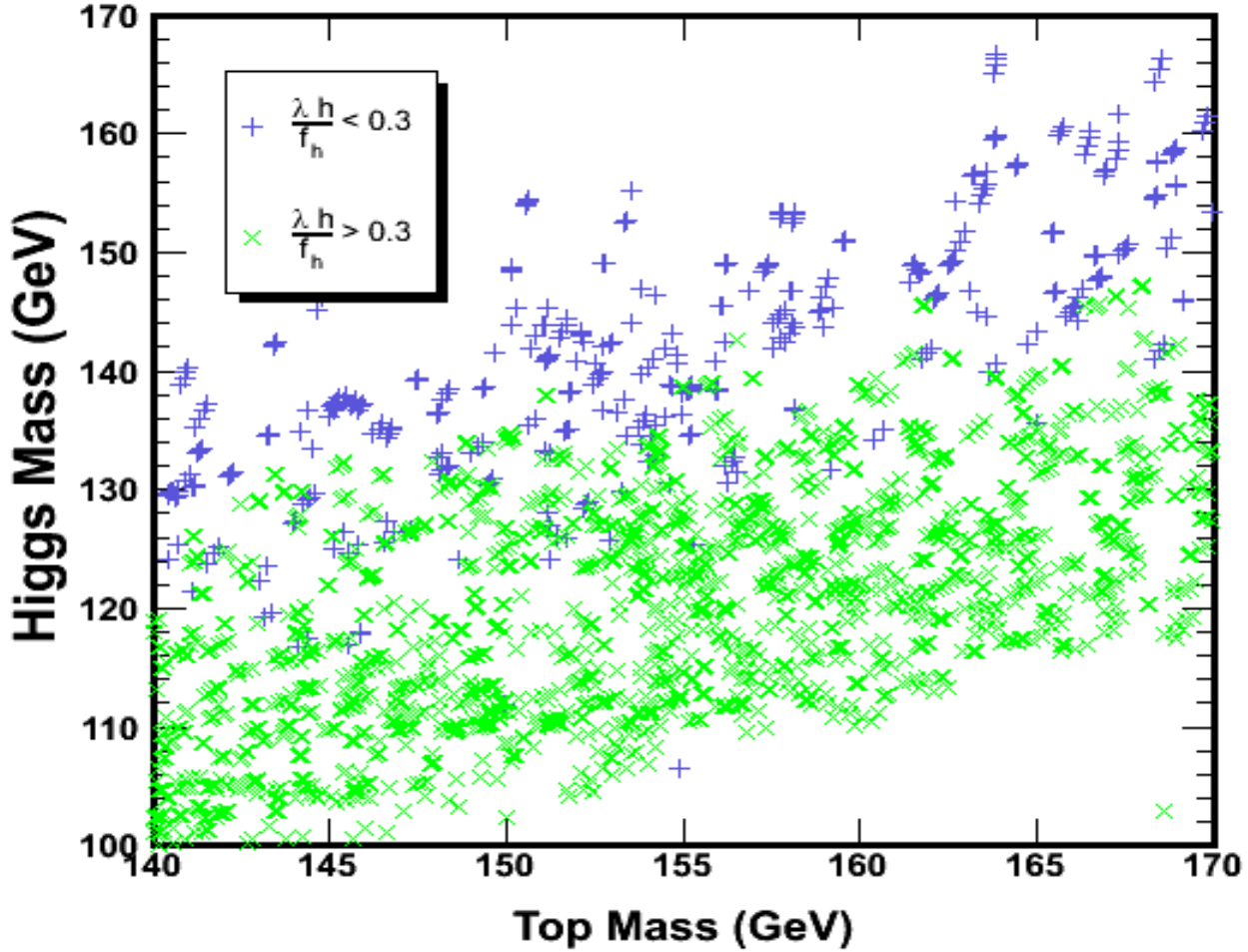


Figure 2: Higgs Mass vs top mass in GeV, zoomed in region. Blue (dark gray) crosses represent the linear regime, green (light gray) x's the non-linear regime.

the second derivative of the effective potential with respect to h , evaluated at the vev. As we will show, somewhat smaller Higgs boson mass values tend to be associated with smaller values of the top quark mass, a reflection of the power dependence of the low-energy Higgs quartic coupling on the top quark mass. The Higgs mass and the KK spectrum are seen to be only weakly dependent on variations of the bottom quark mass in the above defined range.

Although we will display all results consistent with the observed quark and gauge boson low energy spectrum, we will concentrate on points in parameter space in the linear regime, such that $\lambda h/f_h < 0.3$. By linear regime we mean the regime where higher order interactions involving the Higgs field, $\propto (H/\tilde{k})^n$ with $n > 1$, can be neglected and, furthermore, the couplings of the Higgs with gauge bosons and fermions are very close to the ones in the SM. Therefore, in this regime the direct search LEP bounds on the Higgs mass apply, and $m_H \gtrsim 114$ GeV. In addition, the low energy effective theory is well approximated by the SM, with renormalizable couplings and a light Higgs boson. This allow us also to compare our results with those of Ref. [9, 10] where they performed

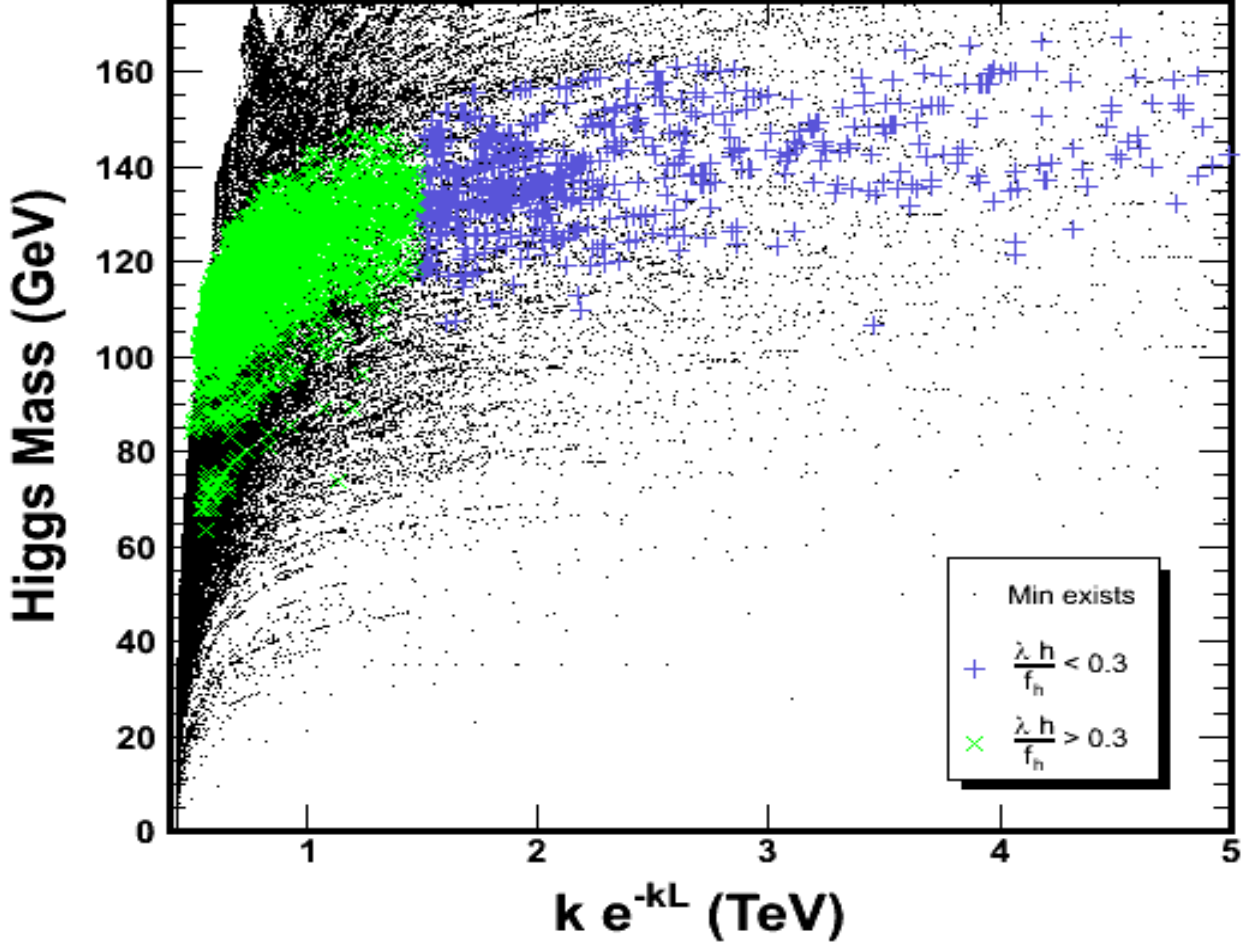


Figure 3: Higgs Mass (GeV) vs \tilde{k} (TeV). Blue (dark gray) crosses represent the linear regime, green (light gray) x's the non-linear regime and black dots where a minimum for the effective potential exists.

calculations in the linear regime as defined above.

We can interpret \tilde{k} as the associated mass scale of our theory and of the order of the natural UV cut off of the low-energy, SM-like effective theory. The scale \tilde{k} is inversely proportional to $\lambda h/f_h$ and therefore as we move away from the linear regime, we are pushing the UV cut-off lower and additionally causing the linear couplings of the Higgs to become smaller. Therefore, the theory becomes increasingly non-renormalizable, which leads to the need of taking into account higher order KK-states (beyond zero-modes) in the calculation of low-energy processes, thus making connection with SM predictions harder. When $\tilde{k} < 2.5$ TeV, KK bosonic and fermionic resonances of exotic and SM fields have a chance to be detected in the next generation colliders such as the LHC; hence, we will be specifically interested in those regions.

We performed two major numerical parameter scans. In the first one we scanned the parameter space for values $c_i \in [-1, 1]$ with $i = 1, 2, 3$ and $M_{B_1}, M_{B_2} \in [0, 5]$. We used $kL = 30$ in our numerical

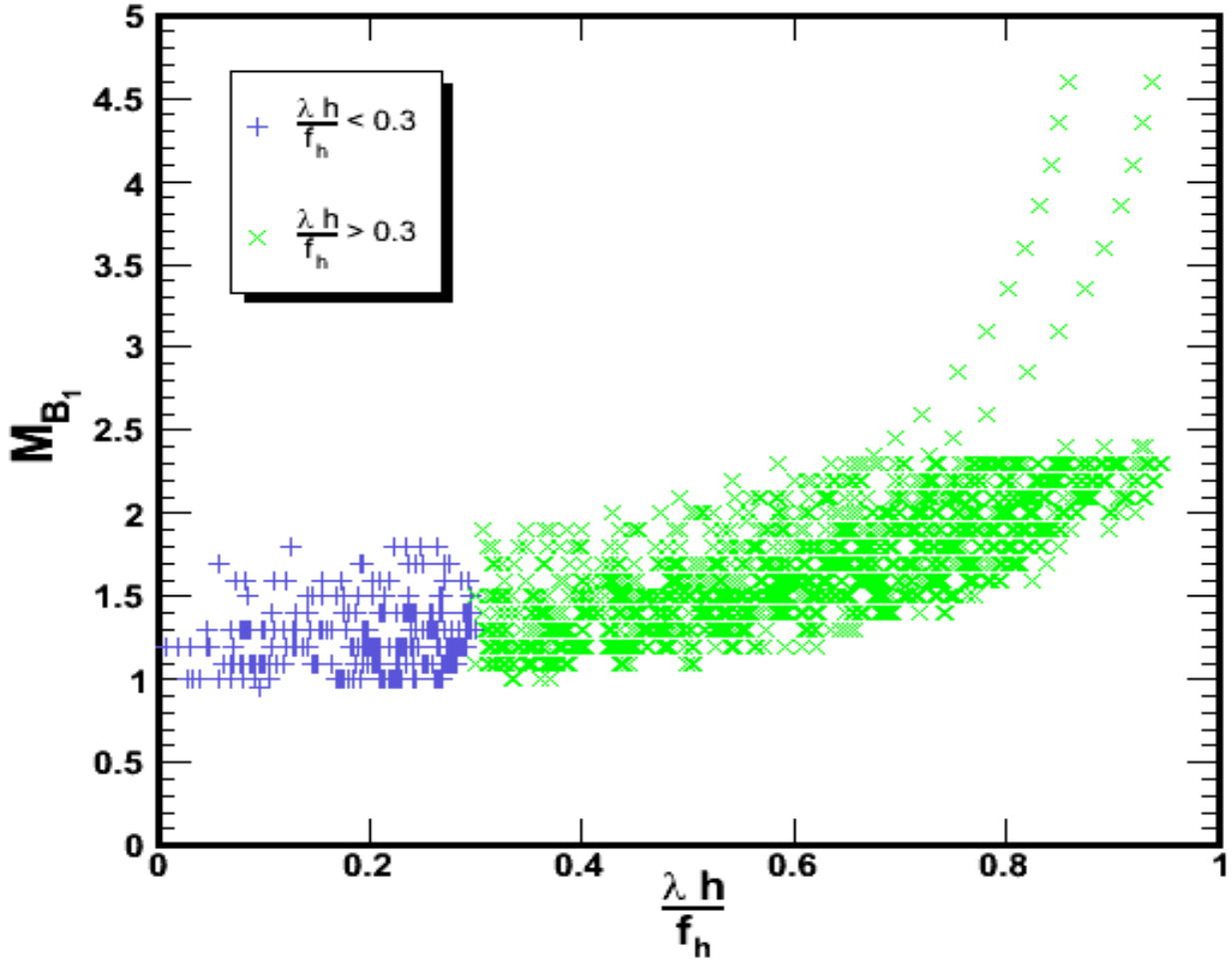


Figure 4: Minimum vs M_{B_1} . Blue (dark gray) crosses represent the linear regime, green (light gray) x's the non-linear regime. The sparse region for higher values of M_{B_1} is due to a coarser grid scanned in that region.

calculations for the masses since the results are invariant under variations of $kL \in [30, 34]$ ². The first scan was done with a coarse grid and before we discuss details of our numerical results, we would like to point out that the effective potential is a completely well behaved function of all the parameters, therefore, we expect that the gaps in our scanned space are smoothly filled. We found that even though for some value of the other parameters, non-trivial minima existed for nearly all the regions of c_i and M_{B_i} , we only found phenomenologically consistent gauge bosons, top and bottom quark masses in the following regions of parameter space: $0 \leq |c_1| \leq 0.3$, $0.35 \leq |c_2| \leq 0.45$, $0.55 \leq |c_3| \leq 0.6$, $1 \lesssim M_{B_1}$ and $M_{B_2} < M_{B_1}$. Though the results show a skew symmetry between positive and negative values, we decided to concentrate on negative values of c_2 and c_3 , since interestingly enough, this is the region which is consistent with electroweak precision measurements [9]. Furthermore, positive values of c_1 lead to a smaller overlap of the left-handed top

²k, obtained from demanding a W-mass in accordance with experiments, adjusts itself so that \tilde{k} remains approximately constant

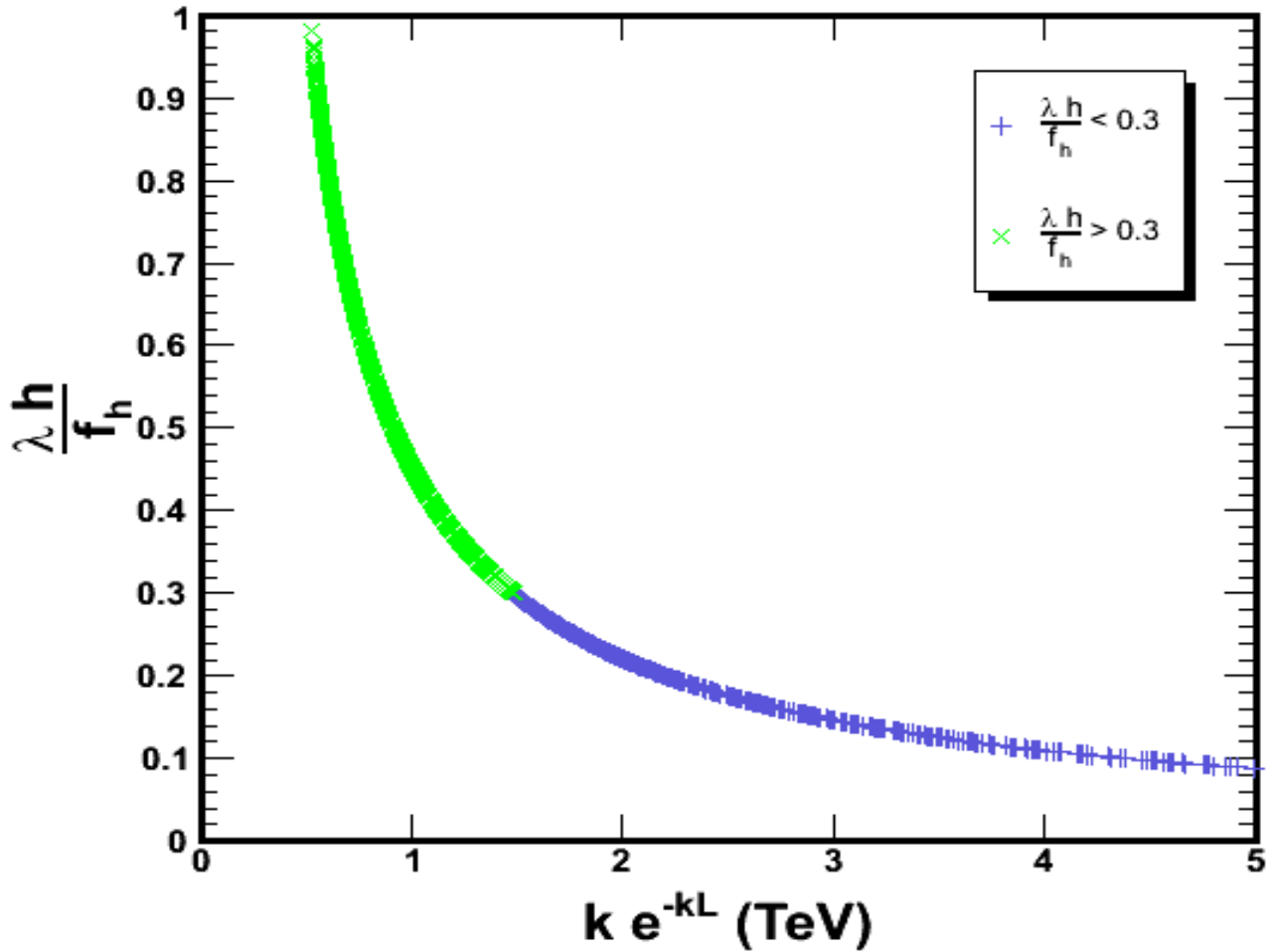


Figure 5: Minimum vs \tilde{k} (TeV). Blue (dark gray) crosses represent the linear regime, green (light gray) x's the non-linear regime

and bottom zero modes with physics at the IR brane, leading to a stronger suppression of potentially dangerous flavor changing operators [20]. Therefore, it is in this region where we performed a more thorough scan taking smaller steps for the c_i .

In Figure 1 we notice a clear relationship between the Higgs and the top-quark masses, where on the plot we have included the bigger coarse scan of parameter space. Focusing on the interesting phenomenological region, we see in Figure 2 that in the linear regime we get Higgs masses that tend to be above 115 GeV, which is above the experimental bound from LEP, and below 160 GeV. Furthermore, there is a somewhat weak dependence of the Higgs mass values on the precise value of the running top quark mass. Higgs mass values closer to the current experimental bound are obtained for the smallest values of the top quark mass in the phenomenologically allowed range. In Figure 3, we manifestly see that in the linear regime we may obtain masses for the Higgs which are compatible with $1.5 \text{ TeV} \lesssim \tilde{k} \lesssim 2.5 \text{ TeV}$.

Figure 4 provides us with information about the 5D parameter M_{B_1} which as increased moves

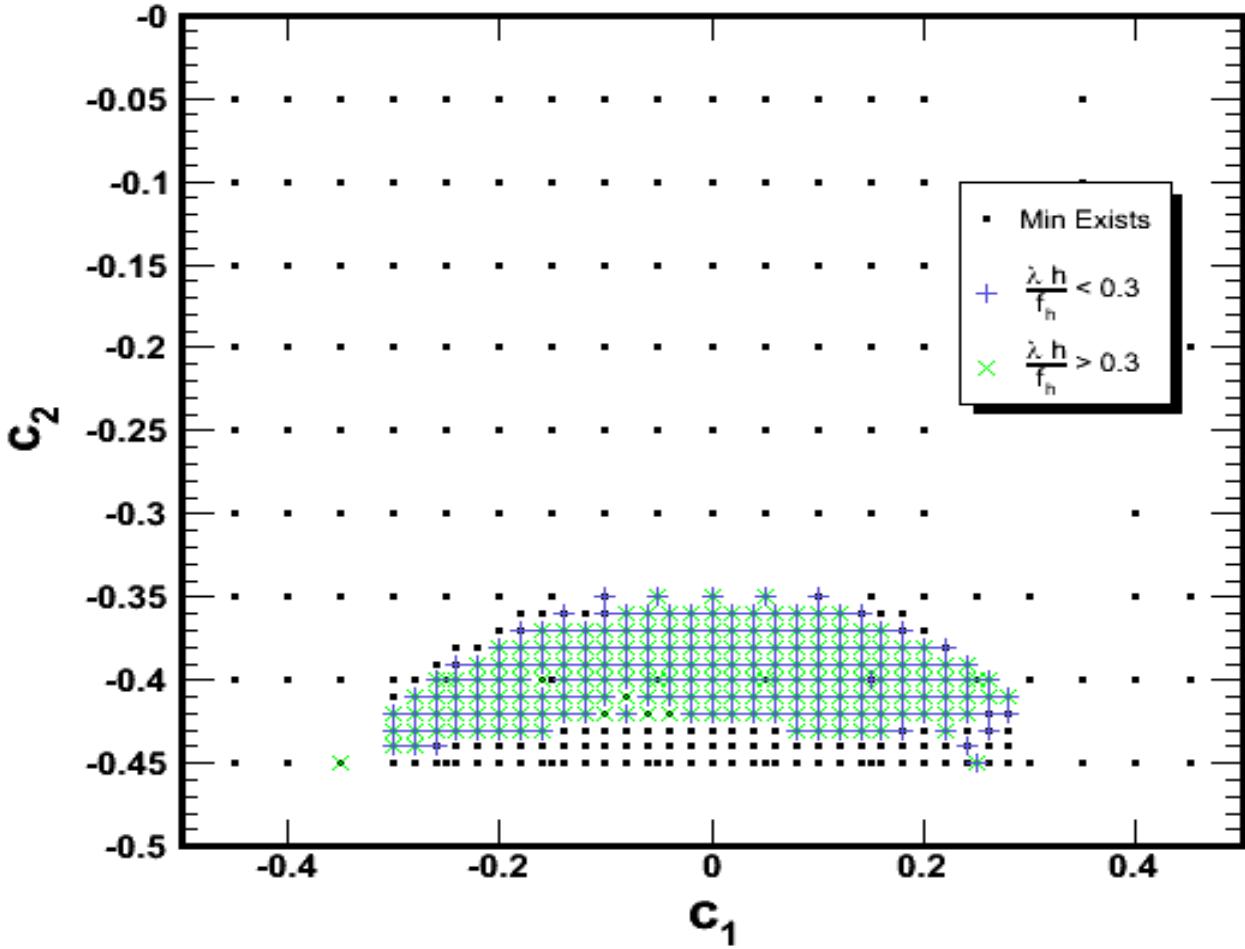


Figure 6: c_1 vs c_2 . Blue (dark gray) crosses represent the linear regime, green (light gray) x's the non-linear regime and black dots where a minimum for the effective potential exists.

the minimum to higher values of $\lambda h/f_h$, getting into the non-linear regime. We conclude that to remain in the linear regime, we cannot have an arbitrarily high M_{B_1} boundary mass parameter.

The behavior $f_h \propto 1/\tilde{k}$ is seen in Figure 5 where, moreover, we notice that for the linear regime, values of $\tilde{k} \gtrsim 1.5$ TeV are obtained. This low value of \tilde{k} will lead to interesting phenomenology for the decays of light KK-fermions and KK-bosons.

In Figure 6 we see that a selected region of the plane $c_1 - c_2$ is suitable for minimizing the effective potential with the experimentally observed W , Z , top and bottom masses, and that the linear regime basically applies through out this region. As emphasized before, $c_1 \gtrsim 0$ and $c_2 \lesssim -0.4$ are the ones preferred by consistency with electroweak precision measurements [9]. In Figure 7 we noticed that the same phenomenologically accepted region for c_2 in the $c_2 - c_3$ plane with $-0.6 \leq c_3 \leq -0.55$ is chosen and it is also homogenously covered in the linear regime.

Figures 8 and 9 are very interesting for collider phenomenology and therefore deserve special attention. Even though we haven't included the plot, we calculated the mass of the W first excited

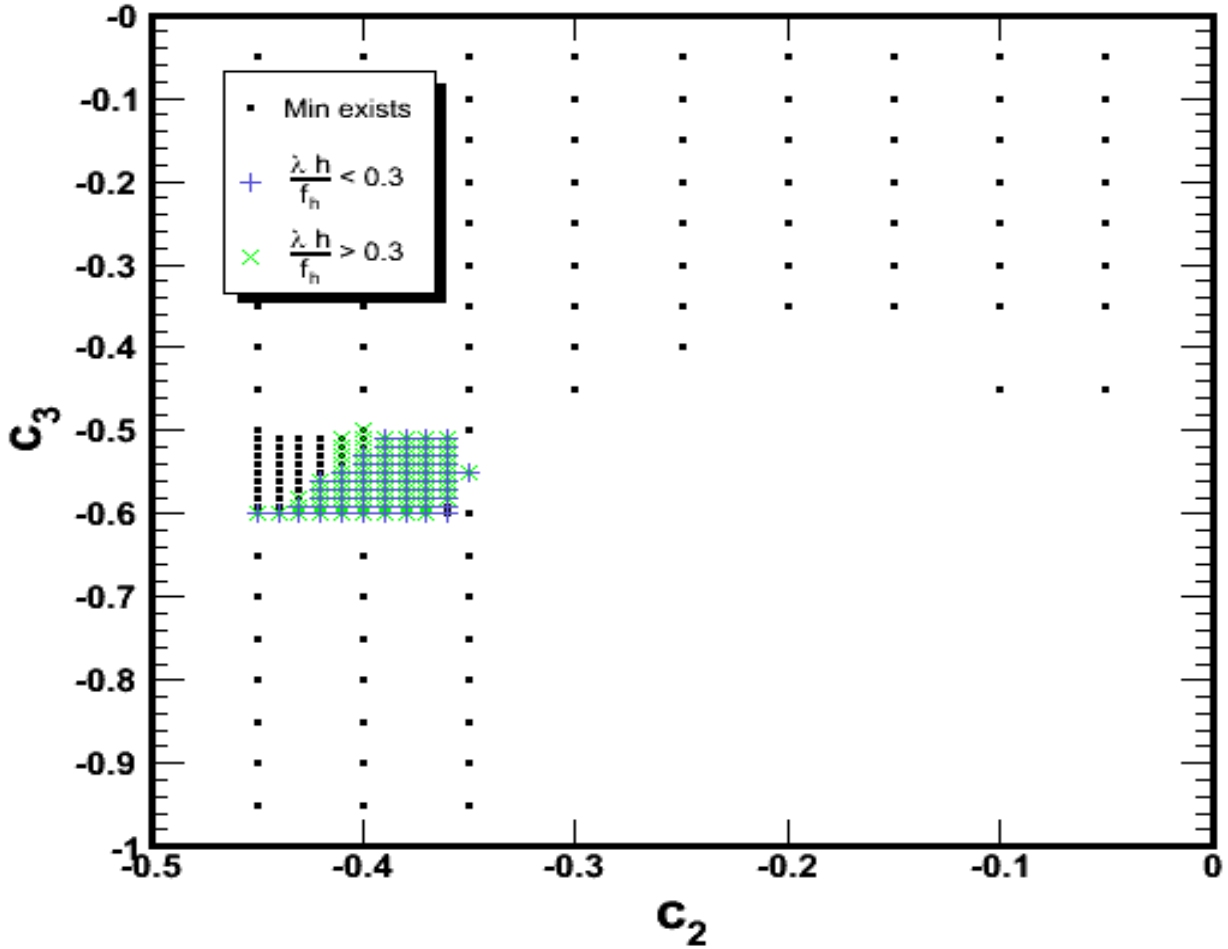


Figure 7: c_2 vs. c_3 . Blue (dark gray) crosses represent the linear regime, green (light gray) x's the non-linear regime and black dots where a minimum for the effective potential exists.

KK state numerically and verified the relation $m_{W^1} \approx 2.5 \tilde{k}$. If the masses of these fermions are below the black line denoting $m_{W^1}/2$, the decay of W^1 and Z^1 to pairs of these fermions is kinematically available. Note here however, that for $c_1 > 0$, $m_{E_1^1}$ is always greater than $m_{W^1}/2$. Moreover, these exotic fermions are unstable. The decay products of T^1 are analyzed in Ref. [10]. The first top KK excited state, will mainly decay to Zt , Ht , Wb . The charged 5/3 fermions of E_1^1 will necessarily decay to Wt from charge conservation, leading to interesting phenomenology [21]. In addition, the lightest KK quark state T^1 , the top quark (via its right- and left-handed couplings) and the bottom quark (via its left-handed coupling) will be included in the KK gluon decay products. This is a distinctive feature of this model when compared with the predominant decay into right-handed top quarks in the models considered in Refs. [22],[23].

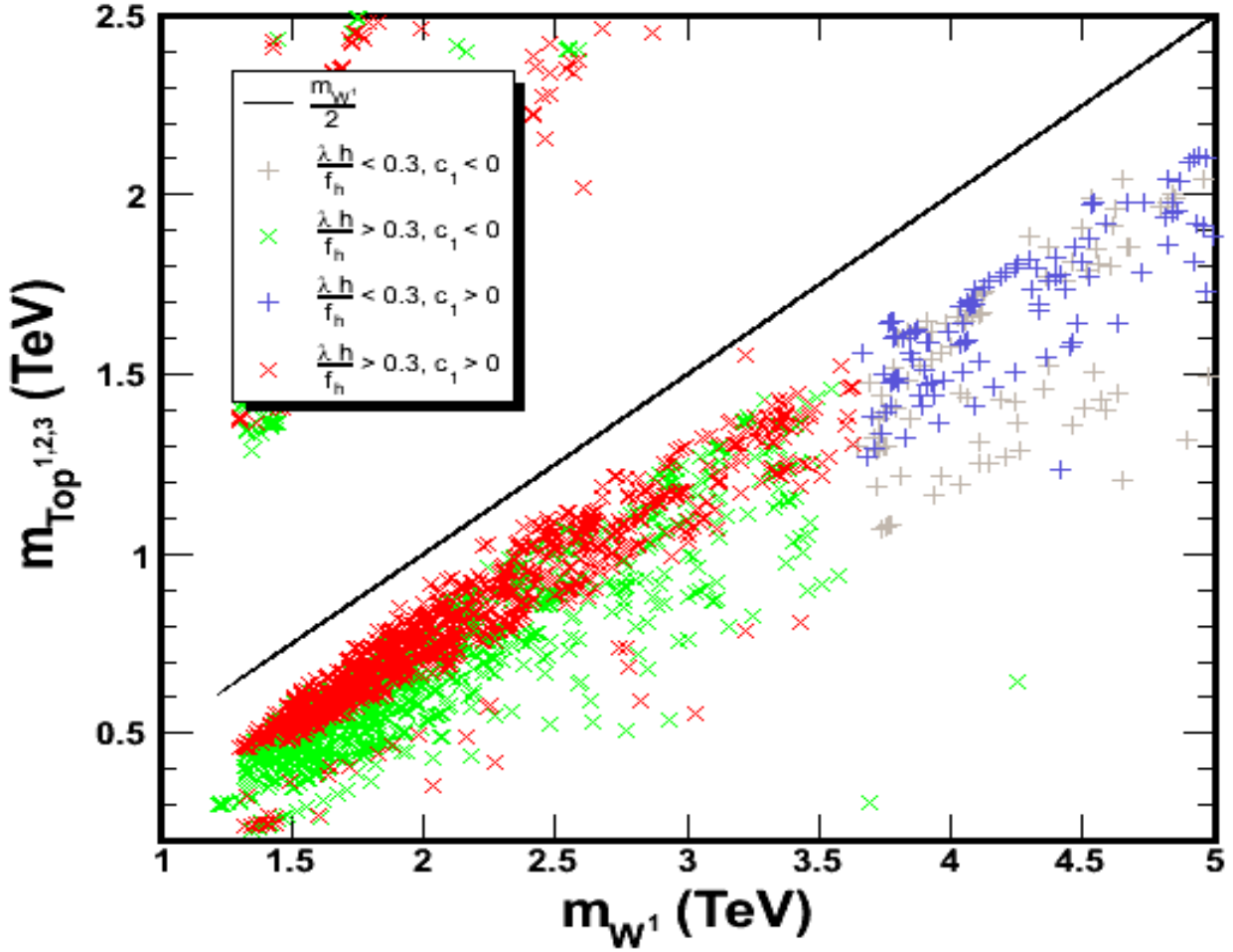


Figure 8: m_{W^1} vs $m_{Top^{1,2,3}}$ in TeV. Also marked is $m_{W^1}/2$ showing that only the first excited top mode can decay into gauge bosons. Blue (dark gray) crosses represent the linear regime with $c_1 > 0$, gray (light gray) crosses the linear regime with $c_1 < 0$, red x's (dark gray) the non-linear regime with $c_1 > 0$, green x's (light gray) the non-linear with $c_1 < 0$.

6 Conclusions

In this article, we computed the one-loop Coleman Weinberg potential for the Higgs field in a specific model of Gauge-Higgs unification in warped extra dimensions. We chose the specific group $SO(5) \times U(1)_X$, which allows the introduction of custodial symmetries protecting the precision electroweak observables as well as a Higgs field with the proper quantum numbers under the electroweak gauge groups. As a first step, we computed the spectral functions of the fermions and gauge bosons of the theory when the Higgs field acquires a vev. These are then used to calculate the effective potential for the Higgs. We demand non-trivial minima that lead to the proper values of the gauge boson and fermion masses in the low energy theory. This requirement leads to a selection of a restricted region of parameters. Interestingly enough, the selected regions of parameters coincide with the ones

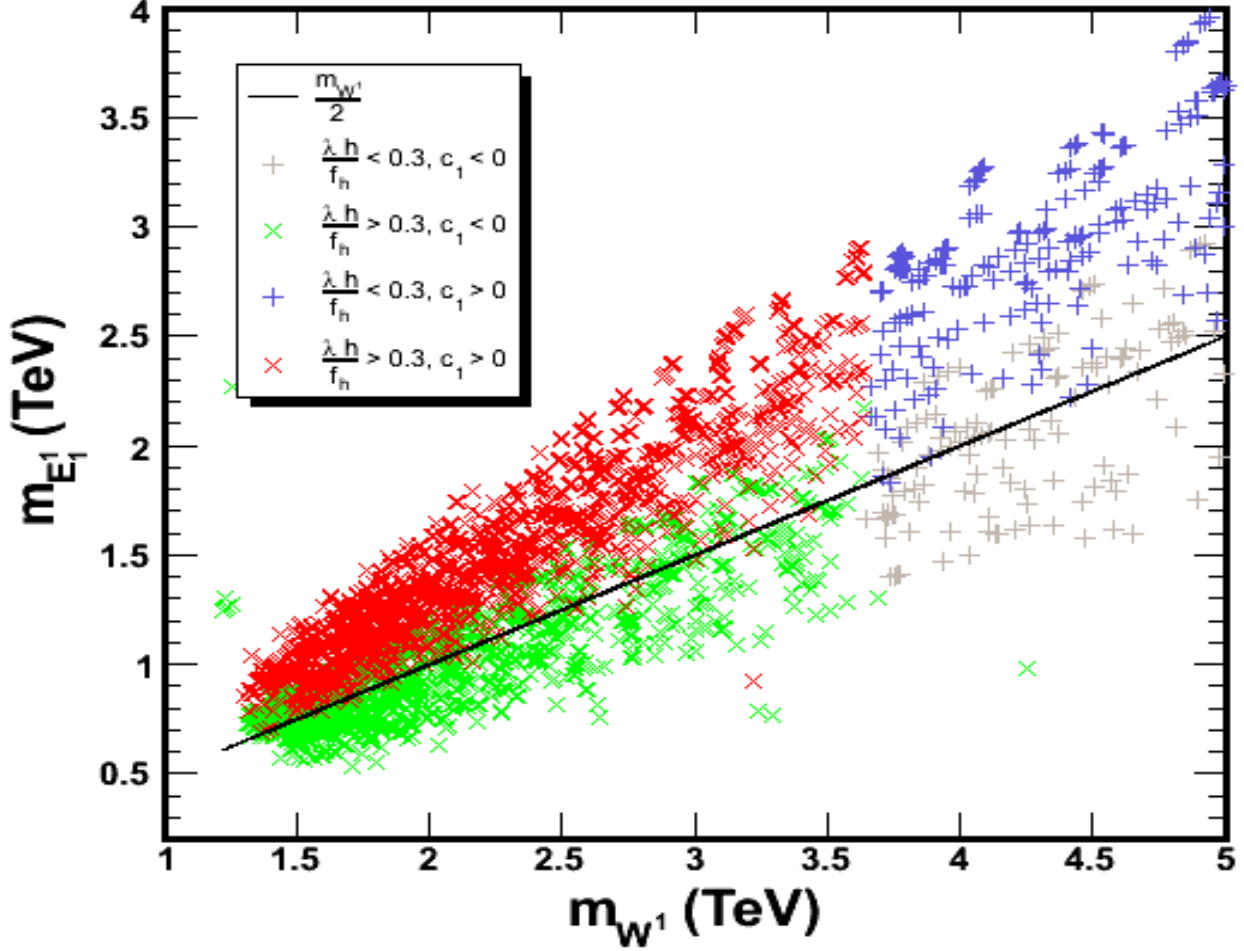


Figure 9: m_{W_1} vs m_{E_1} in TeV. Also marked is $m_{W_1}/2$ showing that depending on the value of the parameters (c_i and B_i) the first mode of the lightest exotic fermion may decay into the gauge bosons. Blue (dark gray) crosses represent the linear regime with $c_1 > 0$, gray (light gray) crosses the linear regime with $c_1 < 0$, red x's (dark gray) the non-linear regime with $c_1 > 0$, green x's (light gray) the non-linear with $c_1 < 0$.

previously selected in order to obtain good agreement with the precision electroweak observables.

Our main result is the computation of the Higgs and KK mass spectra. Demanding that the KK gauge bosons be accessible at the LHC and also that the effective potential minimum be in the linear regime associated with a SM-like low energy effective theory, we obtain Higgs boson masses which are between the present experimental bound on this quantity and about 160 GeV. This range of masses will be tested first at the Tevatron and then at the LHC collider in the near future.

The KK fermion spectrum also shows interesting features. We find that there are KK fermions which become much lighter than the KK gauge bosons. In particular, the lightest KK mode of the top becomes light enough so that the KK gauge bosons will decay into it. There is an additional light KK fermion, which may become light enough for the gauge KK bosons to decay into it, which has exotic quantum numbers under hypercharge, leading for instance to the presence of a light

fermion with charge $5/3e$ with interesting phenomenological properties.

Acknowledgements

We would like to thank Debajyoti Choudhury, Ben Lillie, Arjun Menon, Jing Shu, Tim Tait and particularly Marcela Carena, Eduardo Ponton and Jose Santiago for useful discussions and comments. Work at ANL is supported in part by the US DOE, Div. of HEP, Contract DE-AC02-06CH11357. This work was also supported in part by the U.S. Department of Energy through Grant No. DE-FG02-90ER40560.

APPENDIX

A $SO(5)$ Generators

The generators of the fundamental representation of $SO(5)$, with $\text{Tr}[T^\alpha T^\beta] = C(5)\delta^{\alpha\beta}$, are given by:

$$\begin{aligned} T_{i,j}^{a_{L,R}} &= -\frac{i\sqrt{C(5)}}{2} \left[\frac{1}{2}\epsilon^{abc}(\delta_i^b\delta_j^c - \delta_j^b\delta_i^c) \pm (\delta_i^a\delta_j^4 - \delta_j^a\delta_i^4) \right], \\ T_{i,j}^{\hat{a}} &= -i\sqrt{\frac{C(5)}{2}}(\delta_i^{\hat{a}}\delta_j^5 - \delta_j^{\hat{a}}\delta_i^5), \end{aligned} \quad (\text{A.1})$$

where $T^{\hat{a}}$ ($\hat{a} = 1, 2, 3, 4$) and $T^{a_{L,R}}$ ($a_{L,R} = 1, 2, 3$) are the generators of $SO(5)/SO(4)$ and $SO(4)$ respectively.

B Fermion Parity Assignments and Brane Masses

Since the Higgs has positive parity, in order to preserve the Z_2 orbifold symmetry, we need to ensure that the product of the parities of the fermions coupled via the Higgs is always positive. The Higgs profile is doubly exponentially suppressed on the UV brane, therefore, we will restrict ourselves to discussion of parities on the IR brane.

Concentrating on the parities of the first two multiplets given in Eq. (24), we notice that the product of the fermion parities coupled by the Higgs is not positive. One way to fix this would be to switch the parities for the $SO(4)$ singlet components:

$$[+, -] \quad \Leftrightarrow \quad [+, +]. \quad (\text{B.1})$$

Due to the introduction of the brane mass terms as in Eq. (25), and looking at Eq. (44) we note that the switch in parity is exactly equivalent to taking $M_{B_1}^2 \rightarrow 1/M_{B_1}^2$. Thus the physical results presented in this work are invariant under the switch of parity with just the above mentioned change in M_{B_1} .

Another way to understand the realization of the Z_2 symmetry is via the spurion formalism. We introduce a spurion field transforming in the fundamental representation of $SO(5)$, and acquiring a very large vev in the $SO(4)$ singlet direction, breaking the $SO(5)$ gauge symmetry to $SO(4)$ on the IR brane. We also introduce local fermionic degrees of freedom on the brane and write large local mass terms involving the spurion, between these degrees of freedom and the ones propagating in the bulk. The fermion parities are chosen to be those preserving Z_2 . By using a procedure similar to the one outlined in Eqs. (26), (27) and (28), we can now change the bulk fermion IR boundary conditions while preserving Z_2 to give the model we are considering in this work. This mechanism would allow us to change the IR boundary conditions not just of the $SO(4)$ singlet fields in the **5**'s, but also of the bidoublets in the **5**'s or in the **10**. For the case of the $SO(4)$ singlet fields in the **5**'s,

we need to add $SO(5)$ singlet fermions on the IR brane, that couple to the $\mathbf{5}$'s via the spurion field. For the case of the bidoublets in the $\mathbf{10}$ or in the $\mathbf{5}$'s, we need to add local $\mathbf{5}$'s and singlet fermions on the IR brane, and couple them appropriately to the bulk $\mathbf{10}$ or $\mathbf{5}$'s via gauge invariant masses or couplings to the spurion field ($SO(5)$ singlet fields are necessary to remove unwanted degrees of freedom). In this way, one could start with the opposite IR parities for the three bidoublets to the ones given in Eq. (24), thus preserving the Z_2 symmetry, and reach the choice of bulk fermion boundary conditions used in this work.

The same spurion mechanism can be used to write the brane mass terms in Eq. (25) in an $SO(5)$ invariant way. A spurion field which is a $\mathbf{5}$ under $SO(5)$, can be used to write the bidoublet-bidoublet mixing brane mass term, M_{B_2} , between the $\mathbf{5}$ and the $\mathbf{10}$ multiplets. The spurion field is coupled to these two via a Yukawa type interaction which can be adjusted to give $M_{B_2} \sim \mathcal{O}(1)$. This field can be the same as the one that is used to change the parities of the fermions as described in the last paragraph. The same procedure, but now using a $\mathbf{15} \equiv \mathbf{14} \oplus \mathbf{1}$ of $SO(5)$ can be used to generate the mass mixing terms between the singlets, M_{B_1} . The $\mathbf{15}$ required can be thought of as arising from a tensor product of the $\mathbf{5}$ spurion field: $\mathbf{5} \otimes \mathbf{5} \equiv \mathbf{10} \oplus \mathbf{14} \oplus \mathbf{1}$. Note that this mechanism will not generate a localized bare mass for the Higgs due to gauge invariance.

C Flip Parities for Q_{2R} and the Introduction of M_{B_3}

We also studied the effects of flipping the parities of Q_{2R} as was done in the context of Ref. [10]. In this case, the parity assignments for the rest of our fermionic content remains the same except for Q_{2R} which now takes the form,

$$Q_{2R} = \begin{pmatrix} \chi_{2R}^{u_i}(+, -)_{5/3} & q_R^{u_i}(+, -)_{2/3} \\ \chi_{2R}^{d_i}(+, -)_{2/3} & q_R^{d_i}(+, -)_{-1/3} \end{pmatrix}. \quad (\text{C.1})$$

If we keep the same boundary mass terms as in Eq. (25) and calculate the fermionic spectral functions we obtain,

$$\tilde{S}_{M_2}^4 = 0 \quad (\text{C.2})$$

$$\tilde{S}_{-M_3}^{\prime 5} = 0 \quad (\text{C.3})$$

$$\left[M_{B_2}^2 \tilde{S}_{M_1} \tilde{S}_{-M_3} + \dot{\tilde{S}}_{M_1} \dot{\tilde{S}}_{-M_3} \right]^2 = 0 \quad (\text{C.4})$$

$$2\tilde{S}_{M_3} \left[M_{B_2}^2 \tilde{S}_{-M_3} \dot{\tilde{S}}_{-M_1} + \tilde{S}_{-M_1} \dot{\tilde{S}}_{-M_3} \right] - M_{B_2}^2 \dot{\tilde{S}}_{-M_1} \sin^2 \left(\frac{\lambda_F h}{f_h} \right) = 0 \quad (\text{C.5})$$

$$\begin{aligned} & 2 \left[M_{B_2}^2 \tilde{S}_{-M_3} \left(-\tilde{S}_{M_2} + \tilde{S}_{M_1} \tilde{S}_{M_2} \tilde{S}_{-M_1} + M_{B_1}^2 \tilde{S}_{M_1} \dot{\tilde{S}}_{M_2} \dot{\tilde{S}}_{-M_1} \right) + \right. \\ & \quad \left. \tilde{S}_{-M_1} \left(\tilde{S}_{M_2} \dot{\tilde{S}}_{M_1} + M_{B_1}^2 \tilde{S}_{M_1} \dot{\tilde{S}}_{M_2} \right) \dot{\tilde{S}}_{-M_3} \right] \\ & + \left(M_{B_2}^2 \tilde{S}_{M_2} \tilde{S}_{-M_3} - M_{B_1}^2 \dot{\tilde{S}}_{M_2} \dot{\tilde{S}}_{-M_3} \right) \sin^2 \left(\frac{\lambda_F h}{f_h} \right) = 0 \end{aligned} \quad (\text{C.6})$$

From these expressions we expect that the only non-trivial EW breaking vacua will be generated when $\lambda_F h / f_h = \pi/2$ which, as discussed in section 5, leads to a theory which is highly non-renormalizable. We performed limited numerical analysis which confirmed this expectation.

For completeness and as a reference for future work we write the expression for the determinant in the case of a non-zero mass mixing boundary term M_{B_3} as in Eq. (25). For simplicity, we turn off the singlet mass mixing M_{B_1} . Keeping parities as in our original model, we derive the following fermionic spectral functions,

$$\dot{\tilde{S}}_{-M_3}^5 = 0 \quad (\text{C.7})$$

$$\left[M_{B_2}^2 \tilde{S}_{M_1} \tilde{S}_{-M_3} \dot{\tilde{S}}_{-M_2} + M_{B_3}^2 \tilde{S}_{M_1} \tilde{S}_{-M_2} \dot{\tilde{S}}_{-M_3} + \dot{\tilde{S}}_{M_1} \dot{\tilde{S}}_{-M_2} \dot{\tilde{S}}_{-M_3} \right] = 0 \quad (\text{C.8})$$

$$2\tilde{S}_{M_3} \left[M_{B_2}^2 \tilde{S}_{-M_3} \dot{\tilde{S}}_{-M_1} \dot{\tilde{S}}_{-M_2} + M_{B_3}^2 \tilde{S}_{-M_2} \dot{\tilde{S}}_{-M_1} \dot{\tilde{S}}_{-M_3} + \tilde{S}_{-M_1} \dot{\tilde{S}}_{-M_2} \dot{\tilde{S}}_{-M_3} \right] - M_{B_2}^2 \dot{\tilde{S}}_{-M_1} \dot{\tilde{S}}_{-M_2} \sin^2 \left(\frac{\lambda_F h}{f_h} \right) = 0 \quad (\text{C.9})$$

$$\begin{aligned} & 2\tilde{S}_{M_2} \left[M_{B_2}^4 \tilde{S}_{M_1} \tilde{S}_{-M_3}^2 \dot{\tilde{S}}_{M_1} \dot{\tilde{S}}_{-M_1} \dot{\tilde{S}}_{-M_2}^2 + M_{B_2}^2 \tilde{S}_{-M_3} \dot{\tilde{S}}_{-M_2} \left(2M_{B_3}^2 \tilde{S}_{M_1} \tilde{S}_{-M_2} \dot{\tilde{S}}_{M_1} \dot{\tilde{S}}_{-M_1} + \right. \right. \\ & \quad \left. \left. \left(-1 + 2\tilde{S}_{M_1} \tilde{S}_{-M_1} \right) \dot{\tilde{S}}_{M_1} \dot{\tilde{S}}_{-M_2} \right) \dot{\tilde{S}}_{-M_3} + \right. \\ & \quad \left. \left(M_{B_3}^4 \tilde{S}_{M_1} \tilde{S}_{-M_2}^2 \dot{\tilde{S}}_{M_1} \dot{\tilde{S}}_{-M_1} + M_{B_3}^2 \left(-1 + 2\tilde{S}_{M_1} \tilde{S}_{-M_1} \right) \tilde{S}_{-M_2} \dot{\tilde{S}}_{M_1} \dot{\tilde{S}}_{-M_2} + \tilde{S}_{-M_1} \dot{\tilde{S}}_{M_1}^2 \dot{\tilde{S}}_{-M_2}^2 \right) \dot{\tilde{S}}_{-M_3}^2 \right] \\ & \quad + \left(M_{B_2}^4 \tilde{S}_{M_1} \tilde{S}_{M_2} \tilde{S}_{-M_3}^2 \dot{\tilde{S}}_{-M_2}^2 + M_{B_2}^2 \tilde{S}_{-M_3} \dot{\tilde{S}}_{-M_2} \left(\tilde{S}_{M_2} \dot{\tilde{S}}_{M_1} \dot{\tilde{S}}_{-M_2} \right. \right. \\ & \quad \left. \left. - 2M_{B_3}^2 \tilde{S}_{M_1} \left(\tilde{S}_{M_2} (-2 + \tilde{S}_{M_1} \tilde{S}_{-M_1}) \tilde{S}_{-M_2} - \dot{\tilde{S}}_{-M_1} \dot{\tilde{S}}_{M_1} \dot{\tilde{S}}_{M_2} \dot{\tilde{S}}_{-M_2} \right) \right) \dot{\tilde{S}}_{-M_3} \right. \\ & \quad \left. + M_{B_3}^2 \left(M_{B_3}^2 \tilde{S}_{M_1} \tilde{S}_{-M_2} \left(2 - 2\tilde{S}_{M_1} \tilde{S}_{-M_1} + \tilde{S}_{M_2} \tilde{S}_{-M_2} \right) + \dot{\tilde{S}}_{M_1} \dot{\tilde{S}}_{-M_2} \left(-2\tilde{S}_{M_2} \tilde{S}_{-M_2} \dot{\tilde{S}}_{M_1} \dot{\tilde{S}}_{-M_1} + \right. \right. \right. \\ & \quad \left. \left. \left. \tilde{S}_{M_1} \tilde{S}_{-M_1} \dot{\tilde{S}}_{M_2} \dot{\tilde{S}}_{-M_2} + \dot{\tilde{S}}_{M_1} \dot{\tilde{S}}_{M_2} \dot{\tilde{S}}_{-M_1} \dot{\tilde{S}}_{-M_2} \right) \right) \dot{\tilde{S}}_{-M_3}^2 \right) \sin^2 \left(\frac{\lambda_F h}{f_h} \right) \\ & \quad \left. - M_{B_3}^2 \dot{\tilde{S}}_{-M_3} (M_{B_2}^2 \tilde{S}_{M_1} \tilde{S}_{-M_3} \dot{\tilde{S}}_{-M_2} + (M_{B_3}^2 \tilde{S}_{M_1} \tilde{S}_{-M_2} + \dot{\tilde{S}}_{M_1} \dot{\tilde{S}}_{-M_2}) \dot{\tilde{S}}_{-M_3}) \sin^4 \left(\frac{\lambda_F h}{f_h} \right) \right] = 0 \quad (\text{C.10}) \end{aligned}$$

Due to the term proportional to $\sin^4(\lambda_F h/f_h)$, we expect to have EWSB in this case, with non-trivial minima that for some region of parameter space could lie in the linear regime as in the model studied in this work.

References

- [1] R. Barate *et al.* [LEP Working Group for Higgs boson searches], Phys. Lett. B **565**, 61 (2003) [arXiv:hep-ex/0306033].
- [2] L. Randall and R. Sundrum, Phys. Rev. Lett. **83**, 3370 (1999) [arXiv:hep-ph/9905221].
- [3] Y. Grossman and M. Neubert, Phys. Lett. B **474**, 361 (2000) [arXiv:hep-ph/9912408].
- [4] S. J. Huber and Q. Shafi, Phys. Lett. B **498**, 256 (2001) [arXiv:hep-ph/0010195].

- [5] N. S. Manton, Nucl. Phys. B **158**, 141 (1979); Y. Hosotani, Phys. Lett. B **126**, 309 (1983); H. Hatanaka, T. Inami and C. S. Lim, Mod. Phys. Lett. A **13**, 2601 (1998) [arXiv:hep-th/9805067]; I. Antoniadis, K. Benakli and M. Quiros, New J. Phys. **3**, 20 (2001) [arXiv:hep-th/0108005]; M. Kubo, C. S. Lim and H. Yamashita, Mod. Phys. Lett. A **17**, 2249 (2002) [arXiv:hep-ph/0111327]; G. von Gersdorff, N. Irges and M. Quiros, Nucl. Phys. B **635**, 127 (2002) [arXiv:hep-th/0204223]; C. Csaki, C. Grojean and H. Murayama, Phys. Rev. D **67**, 085012 (2003) [arXiv:hep-ph/0210133]; N. Haba, M. Harada, Y. Hosotani and Y. Kawamura, Nucl. Phys. B **657**, 169 (2003) [Erratum-ibid. B **669**, 381 (2003)] [arXiv:hep-ph/0212035]; C. A. Scrucca, M. Serone and L. Silvestrini, Nucl. Phys. B **669**, 128 (2003) [arXiv:hep-ph/0304220]; C. A. Scrucca, M. Serone, L. Silvestrini and A. Wulzer, JHEP **0402**, 049 (2004) [arXiv:hep-th/0312267]; N. Haba, Y. Hosotani, Y. Kawamura and T. Yamashita, Phys. Rev. D **70**, 015010 (2004) [arXiv:hep-ph/0401183]; C. Biggio and M. Quiros, Nucl. Phys. B **703**, 199 (2004) [arXiv:hep-ph/0407348]; Y. Hosotani, S. Noda and K. Takenaga, Phys. Lett. B **607**, 276 (2005) [arXiv:hep-ph/0410193]; G. Cacciapaglia, C. Csaki and S. C. Park, JHEP **0603**, 099 (2006) [arXiv:hep-ph/0510366]; G. Panico, M. Serone and A. Wulzer, Nucl. Phys. B **739**, 186 (2006) [arXiv:hep-ph/0510373]; G. Panico, M. Serone and A. Wulzer, arXiv:hep-ph/0605292; R. Contino, Y. Nomura and A. Pomarol, Nucl. Phys. B **671**, 148 (2003) [arXiv:hep-ph/0306259].
- [6] H. Davoudiasl, J. L. Hewett and T. G. Rizzo, Phys. Lett. B **473**, 43 (2000) [arXiv:hep-ph/9911262].
- [7] K. Agashe, A. Delgado, M. J. May and R. Sundrum, JHEP **0308**, 050 (2003) [arXiv:hep-ph/0308036].
- [8] K. Agashe, R. Contino, L. Da Rold and A. Pomarol, Phys. Lett. B **641**, 62 (2006) [arXiv:hep-ph/0605341].
- [9] M. Carena, E. Ponton, J. Santiago and C. E. M. Wagner, Nucl. Phys. B **759**, 202 (2006) [arXiv:hep-ph/0607106].
- [10] M. Carena, E. Ponton, J. Santiago and C. E. M. Wagner, arXiv:hep-ph/0701055.
- [11] R. Contino, L. Da Rold and A. Pomarol, Phys. Rev. D **75**, 055014 (2007) [arXiv:hep-ph/0612048].
- [12] A. Falkowski, Phys. Rev. D **75**, 025017 (2007) [arXiv:hep-ph/0610336].
- [13] K. Agashe and R. Contino, Nucl. Phys. B **742**, 59 (2006) [arXiv:hep-ph/0510164].
- [14] K. Agashe, R. Contino and A. Pomarol, Nucl. Phys. B **719**, 165 (2005) [arXiv:hep-ph/0412089].
- [15] Y. Sakamura and Y. Hosotani, Phys. Lett. B **645**, 442 (2007) [arXiv:hep-ph/0607236].
- [16] Y. Hosotani and M. Mabe, Phys. Lett. B **615**, 257 (2005) [arXiv:hep-ph/0503020].

- [17] A. Pomarol, Phys. Lett. B **486**, 153 (2000) [arXiv:hep-ph/9911294].
- [18] M. E. Peskin and T. Takeuchi, Phys. Rev. D **46**, 381 (1992).
- [19] W. M. Yao *et al.* [Particle Data Group], J. Phys. G **33**, 1 (2006).
- [20] T. Gherghetta and A. Pomarol, Nucl. Phys. B **586**, 141 (2000) [arXiv:hep-ph/0003129];
- [21] C. Dennis, M. Karagoz Unel, G. Servant and J. Tseng, arXiv:hep-ph/0701158.
- [22] B. Lillie, L. Randall and L. T. Wang, arXiv:hep-ph/0701166.
- [23] K. Agashe, A. Belyaev, T. Krupovnickas, G. Perez and J. Virzi, arXiv:hep-ph/0612015.